

February 1, 2008

UTTG-08-02
hep-th/0207114

All Genus Topological String Amplitudes and 5-brane Webs as Feynman Diagrams

Amer Iqbal

Theory Group, Department of Physics
University of Texas at Austin,
Austin, TX 78712, U.S.A.

Abstract

A conjecture for computing all genus topological closed string amplitudes on toric local Calabi-Yau threefolds, by interpreting the associated 5-brane web as a Feynman diagram, is given. A propagator and three point vertex is defined which allows us to write down the amplitude associated with 5-brane web. We verify the conjecture that this amplitude is equal to the closed string partition function by computing integer invariants for resolved conifold and certain curves of low degree in local del Pezzo surfaces, local Hirzebruch surfaces and their various blowups.

arXiv:hep-th/0207114v2 12 Jul 2002

1 Introduction

Topological string amplitudes have been of interest to physicists and mathematicians for a long time. For physicists these amplitudes compute terms in the low energy effective action of the theory obtained by compactifying IIA string theory on a Calabi-Yau threefold [1]. They are of interest to mathematicians since they are the generating functions of Gromov-Witten invariants [2, 3] of holomorphic curves in Calabi-Yau threefold [4].

For the case of toric Calabi-Yau threefolds various techniques are available for computing these amplitudes. Localization can be used for a direct calculations in the A-model [5]. This was discussed in detail in [6] for genus zero case using mirror symmetry. Higher genus calculations, using localization, for the local \mathbb{P}^2 case were carried out in [7]. B-model calculation, although tedious, provide another way of calculating these amplitudes up to certain unknown constants which can sometimes be fixed from their behavior at the singular points [8] in the moduli space and using the hidden integrality properties of the invariants [9].

Integer invariants of holomorphic curves in Calabi-Yau threefolds were defined in [10] and it was shown that topological closed string amplitudes when interpreted from the target space point of view are the generating functions of these integer invariants,

$$F(\omega) = \sum_{g=0}^{\infty} g_s^{2g-2} F_g(\omega) = \sum_{m=1}^{\infty} \sum_{\beta \in H_2(X, \mathbf{Z})} \sum_{r=0}^{\infty} \frac{N_{\beta}^r}{m} (2 \sin(m \frac{g_s}{2}))^{2r-2} e^{-m\beta \cdot \omega}. \quad (1)$$

Where X is the Calabi-Yau with Kähler form ω and $N_{\beta}^r \in \mathbf{Z}$ are the invariants. Topological open string amplitudes were reformulated in terms of open string integer invariants in [11] by interpreting them from the target space point of view.

A completely new way of obtaining the topological closed string amplitudes from the Chern-Simons theory was developed in [12] using geometric transition: deformation versus resolution of the singularity. The case of blown up conifold was discussed in detail and all genus closed string amplitude of the blown up conifold was derived from the partition function of the Chern-Simons theory on S^3 . Recently this open-closed duality, Chern-Simons theory being the theory of topological open strings, was proved from the world-sheet point of view [13]. The fact that both open and closed string invariants are related to knot invariants in a geometry obtained via geometric transition has been checked for many cases [14, 15, 16, 17, 19, 20].

Closed string invariants for more complicated geometries, such as local toric del Pezzo surfaces, have been calculated from the Chern-Simons theory using geometric transition [20, 21]. Unlike the case of the resolved conifold, in these cases the Chern-Simons theory on the space obtained after geometric transition gets corrections from the holomorphic curves with boundaries on the 3-cycles [22]. This open-closed duality, Chern-Simons theory being the theory

of open strings [22], has been checked in many cases and is by far the easiest method for calculating the Gromov-Witten invariants and check their hidden integrality properties as formulated in terms of integer invariants [10]

It is well known that knot invariants in the Chern-Simons theory can be calculated using the WZW theory. In this note we conjecture that using the 5-brane web description of toric local Calabi-Yau threefolds [23] the topological closed string partition function can be written directly using the propagator and vertex defined by states and operators in the large N WZW theory. Since the 5-brane web naturally gives rise to a Riemann surface the topological closed string partition function is an amplitude associated with this Riemann surface. The conjecture is motivated by the lattice model interpretation of the topological closed string amplitudes given in [21]. It follows from their discussion once we recognize that the “three point vertex” is more basic than the four point vertex of the lattice model [21] and that all 5-brane web diagrams can be constructed from $(1,0)$ 5-brane (“the propagator”), three point vertex given by $(1,0)$, $(0,1)$ $(1,1)$ 5-branes and their $SL(2, \mathbf{Z})$ transforms. We verify the idea by computing integer invariants, from this 5-brane web amplitude, for various geometries.

Using the 5-brane/7-brane description of certain local Calabi-Yau threefolds, developed in [24] we conjecture the form of closed string partition function for some non-toric threefolds. From the 5-brane/7-brane description of toric local Calabi-Yau threefolds it appears that closed string partition function is given by particular Feynman diagrams in the vacuum to vacuum amplitude. The case of non-toric threefolds will be discussed in more detail elsewhere[18].

This paper is organized as follows. In section two we discuss briefly the 5-brane web description of toric local Calabi-Yau threefolds. We also discuss, in this section, the Riemann surface coming from the 5-brane web when IIB string theory is lifted to M-theory after compactification on a circle. In section two we define the propagator and the three point vertex using the states and the operators of the WZW theory. We also discuss the matrix elements and their computation which will be needed later to work out the integer invariants. The matrix elements we will need are related to the Hopf link with linking number plus one and therefore the discussion of matrix elements is mostly based on section three of [21]. In section three we compute integer invariants for a few curves of low degree in various toric local Calabi-Yau threefolds with a single compact divisor from the 5-brane web description. A more complete account of these invariants for curves of higher degree in these geometries will be given elsewhere [18].

2 Local threefolds and 5-brane webs and the Riemann surface

In this section we discuss toric local Calabi-Yau threefolds, their dual description involving (p, q) 5-branes of type IIB string theory and the Riemann surface associated with the web.

2.1 CY and 5-brane web

The relation between local toric Calabi-Yau spaces and 5-brane webs of type IIB string theory follows from the basic duality between M-theory on T^2 and type IIB string theory on S^1 . Consider as an example the resolved conifold which has a toric description given by the following equation [31],

$$\begin{aligned} |X_1|^2 + |X_2|^2 - |X_3|^2 - |X_4|^2 &= r, \\ (X_1, X_2, X_3, X_4) &= (e^{i\theta} X_1, e^{i\theta} X_2, e^{-i\theta} X_3, e^{-i\theta} X_4). \end{aligned} \quad (2)$$

At a point, where none of X_i are zero we have a $T^4/U(1)$. Where the $U(1)$ acts with

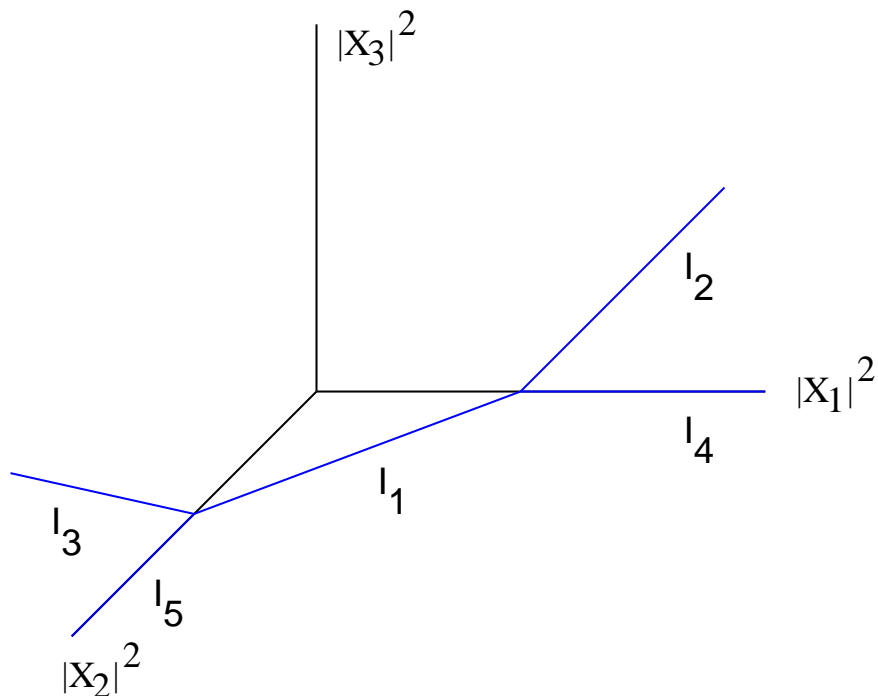


Figure 1: The resolved conifold. Line segments I_a represent different collapsing $U(1)$'s.

charges $(1, 1, -1 - 1)$ on the phases of X_a which form the T^4 . On different line segments I_a , shown in Fig. 1, two different X_a become zero and therefore we are left with a single $U(1)$ after modding out. If we consider the \mathbb{R}^2 orthogonal to the line passing through the origin and making equal angle with all three axis then we get a T^2 fibration over this plane with T^2 degenerating as shown in Fig. 2. On this plane we can choose the directions such

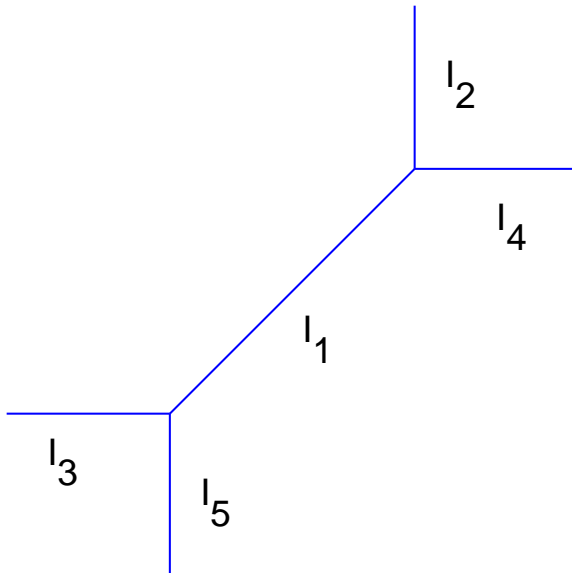


Figure 2: Projection of the resolved conifold.

that (p, q) cycle degenerates along a line segment oriented in the (p, q) direction. Now if we apply M-theory/IIB duality adiabatically we see that the T^2 disappears and its information is encoded in the branes present along the locus of degeneration. The line segment directed in the (p, q) direction, along which (p, q) cycle was degenerating, now has (p, q) 5-brane of IIB string theory.

The 5D $\mathcal{N} = 1$ theory on the transverse space coming from M-theory on the CY is dual to the 5D $\mathcal{N} = 1$ theory on the 5-brane web. By compactifying one direction transverse to the conifold we can go to type IIA string theory on the blown up conifold. Compactifying one of the common directions of the 5-branes we can go back to M-theory with 5-brane web becoming a single M5-brane wrapped on a Riemann surface embedded in $\mathbb{R}^2 \times T^2$. We will see that this Riemann surface plays the central role in writing down the string partition function. This perhaps is related to the results of [27, 28] where relation between string partition functions and M5-brane theory was explored. The Riemann surface projects to \mathbb{R}^2 as a thickened 5-brane web. The $\mathcal{N} = 2$ theory on the transverse space obtained by compactifying type IIA string theory on a local Calabi-Yau threefolds has a dual description as the theory on an M5-brane wrapped on the Riemann surface associated with the corresponding web.

For toric local Calabi-Yau this Riemann surface can easily be obtained from the toric data

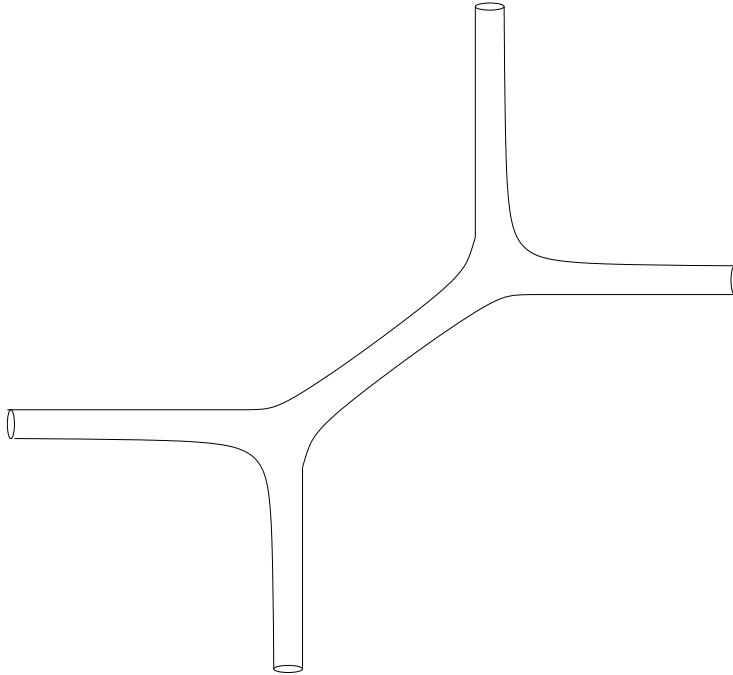


Figure 3: The Riemann surface associated with the 5-brane web dual to the resolved conifold.

and plays an important role in constructing the mirror Calabi-Yau threefold. If the Riemann surface associated with web is given by $f(e^u, e^v) = 0$ (u, v being coordinates on $R^2 \times T^2$) then the mirror Calabi-Yau threefold is given by

$$f(e^u, e^v) = xy, \quad x, y \in \mathbb{C}. \quad (3)$$

3 5-brane webs as Feynman diagrams

5-brane webs provide an interesting way of encoding the geometry of the dual Calabi-Yau threefold. The curves in the CY which give rise to BPS states of the $\mathcal{N} = 1$ 5D theory correspond to (p, q) strings ending on the (p, q) 5-branes of the web. From this web description of curves it is easy to compute the intersection number of curves and also the genus of a curve using the fact that the web of (p, q) strings should be trivalent [25, 23, 26].

The most basic web is the one composed of the $(1, 0)$, $(0, 1)$ and the $(1, 1)$ 5-brane. This web corresponds to the threefold \mathbb{C}^3 as can be seen by taking the limit in which the Kähler parameter of the \mathbb{P}^1 of the resolved conifold goes to infinity. Since we are in type IIB string

theory which has $SL(2, \mathbf{Z})$ symmetry, therefore there is no unique web corresponding to a local toric Calabi-Yau threefold. By an $SL(2, \mathbf{Z})$ transformation $\begin{pmatrix} p & r \\ q & s \end{pmatrix}$ we can map the $(1, 0)$, $(0, 1)$ and $(1, 1)$ web to (p, q) , (r, s) and $(p+q, r+s)$ web. The invariant aspect of this transformed web is the intersection number of the external charges,

$$\det \begin{pmatrix} p & r \\ q & s \end{pmatrix} = 1. \quad (4)$$

If we have a web with three 5-branes meeting a point such that the intersection number of any two of them is not ± 1 then it is possible to resolve into a web with more than one trivalent vertices such that the intersection numbers at both vertices are ± 1 . The fact that the intersection number is not ± 1 is a reflection of the fact that the corresponding CY has a singularity [23]. The resolution of the singularity of the Calabi-Yau is then reflected in the dual web diagram as the appearance of more vertices. A simple example of this is given by the web diagram of the Calabi-Yau which is the total space of $\mathcal{O}(-3)$ bundle over \mathbb{P}^2 . If the \mathbb{P}^2 is shrunk then the CY has a singularity and the web diagram of the singular CY consists of $(-1, 1)$, $(2, 1)$ and $(-1, -2)$ branes. The intersection numbers in this case are ± 3 (depending on the orientation) and therefore the web can be resolved as shown in Fig. 4. It is easy to check that the resolved web has intersection numbers ± 1 at each vertex and

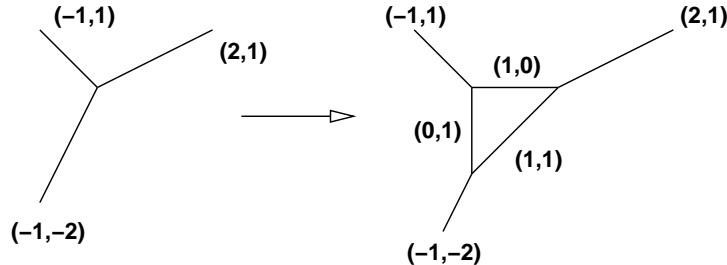


Figure 4: Resolution of $\mathbb{C}^3/\mathbf{Z}_3$.

therefore each vertex is an $SL(2, \mathbf{Z})$ transform of the basic $(1, 0)$, $(0, 1)$ and $(1, 1)$ vertex. Thus we can decompose any web into pieces which are $SL(2, \mathbf{Z})$ transform of the basic three point vertex and the $(1, 0)$ 5-brane as shown in Fig. 5 for the case of resolved conifold and local \mathbb{P}^2 .

In [21] a lattice model interpretation of topological closed string amplitudes was discussed and it was suggested that with a web configuration in which all three point vertices can be converted into four point vertices (in the CY context this corresponds to shrinking \mathbb{P}^1 's with normal bundle $\mathcal{O}(-1) \oplus \mathcal{O}(-1)$) matrix element $\langle \bar{R}_3, \bar{R}_4 | V | R_1, R_2 \rangle$ should be associated with the four point vertices and propagators e^{-lRr} with the edges. Where $|R\rangle$ are the states of the $SU(N)$ WZW theory which are labeled by the highest weight representations R at level

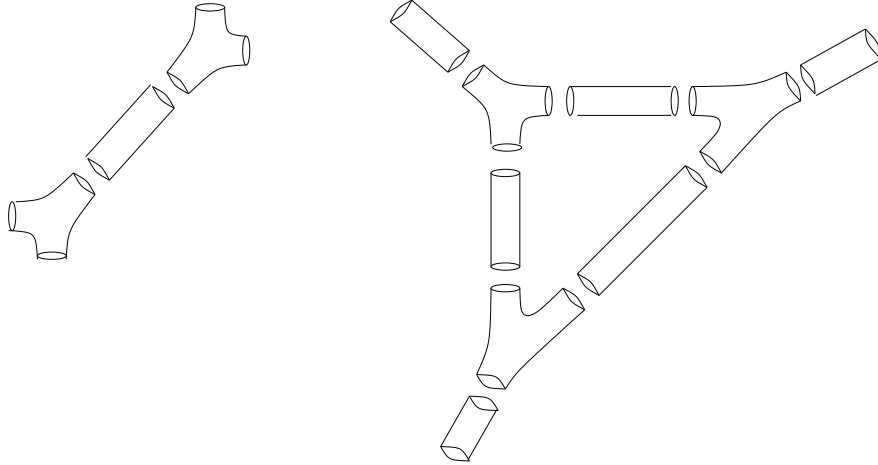


Figure 5: a) Resolved conifold, b) local \mathbb{P}^2 . The Riemann surface associated with the web, and the web itself, can be constructed from two basic objects.

$k + N$ and l_R is the first Casimir of the representation R equal to the number of boxes in the Young-Tableaux of R . r is the length of the edge and is the Kähler parameter of the associated rational curve in the dual Calabi-Yau. In the case of an external edge we have $r \mapsto \infty$ and therefore the state associated with the external legs is the vacuum state $|0\rangle$. As discussed in [21] the state $|R_1, R_2\rangle$ is given by the fusion coefficients,

$$|R_1, R_2\rangle = \sum_R N_{R_1 R_2}^R |R\rangle, \quad (5)$$

where the fusion coefficient are given in terms of the modular S matrix,

$$N_{R_1 R_2}^R = \sum_{R'} \frac{S_{R' R_1} S_{R' R_2} S_{R' R}^{-1}}{S_{0 R'}}. \quad (6)$$

We have seen that three point vertex is more basic than the four point vertex and therefore it is should be possible to associate with it a matrix element $\langle \bar{R}_3 | \mathcal{O} | R_2, 0 \rangle$, with \mathcal{O} being some appropriate operator and $|0\rangle, |R_2\rangle$ states on the incoming circles and $|R_3\rangle$ the state on the outgoing circle as shown in Fig. 6. We always consider the vertices in which one of the boundary circles goes of to infinity so that the state on it is the vacuum state. We take the amplitude for this vertex to be ¹

$$V(\alpha, \beta; \alpha - \beta) := \langle \bar{R}_3 | S^{-1} | R_2, 0 \rangle, \quad (7)$$

where the operator $\mathcal{O} = S^{-1}$ has been chosen such that the corresponding $SL(2, \mathbf{Z})$ matrix takes the incoming circle β into an outgoing circle α .² The importance of the three point

¹I am grateful to Cumrun Vafa for pointing out a mistake in the definition of the vertex in an earlier version of the preprint.

²The Riemann surface is embedded in $\mathbb{R}^2 \times T^2$ and α, β are the basis of $H_1(T^2, \mathbf{Z})$ such that $\alpha \cdot \beta = 1$.

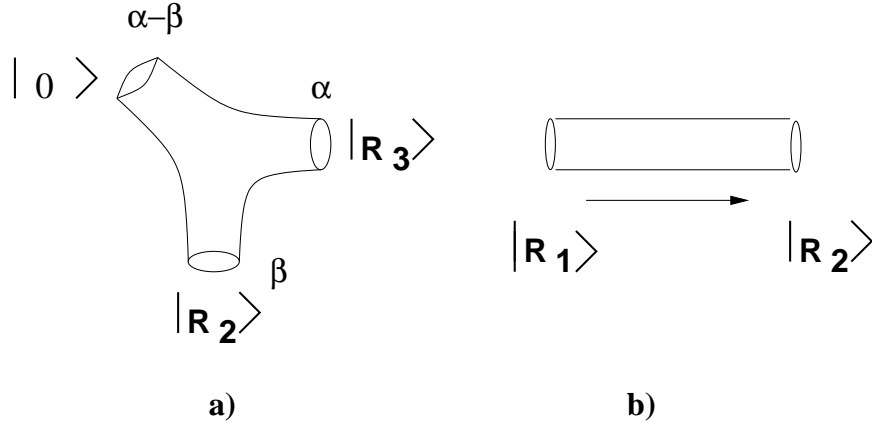


Figure 6: a) The vertex, b) the propagator.

vertex has also been noted in [33] where a vertex with all three circles having non-trivial state has been worked out.

An asymmetrical choice between β and $\alpha - \beta$ was made here. Of the two incoming cycles we choose the one which is followed by the outgoing cycle in the counter clock-wise rotation on the vertex. We will carefully choose our web diagrams from among all $SL(2, \mathbf{Z})$ transforms so that the operators at the vertices are of the form $T^m S^{-1} T^k$ for $m, k \in \mathbf{Z}$. We will see that this is possible for all local del Pezzo surfaces, local Hirzebruch surfaces and their various blowups. This choice is made so that we can use the method given in [21] to calculate the matrix elements $\langle \bar{R} | T^m S^{-1} T^k | R' \rangle$. For the propagator which is cylinder of length r with states $|R_1\rangle$ and $|R_2\rangle$ at the two boundary circles $J_{R_1}, J_{R_2} \in H_1(T^2, \mathbf{Z})$ we choose,

$$P(J_{R_1}, J_{R_2}) := e^{-l_{R_1} r} \delta_{R_1 R_2}. \quad (8)$$

Although not all web diagrams would allow operators at the vertices of the form $T^n S^{-1} T^m$ simultaneously we will restrict ourselves to geometries which do allow such vertices so that we can use the results of [21].

The states and the operators we used to define the propagator and the vertices are that of the $U(N)$ WZW theory. It is well known that the primary field of this theory are associated with highest weight representations at level $k + N$ [32, 34]. A state $|R\rangle$ with weight vector λ_R has conformal dimension

$$h_R = \frac{(\lambda_R, \lambda_R + 2\rho)}{2(k + N)} \quad (9)$$

where ρ is one half the sum of positive roots. These states define an orthonormal basis of the Hilbert space of the Chern-Simons theory on a manifold with boundary of genus one,

$\langle \bar{R}_1 | R_2 \rangle = \delta_{R_1, R_2}$. As discussed in [32] $SL(2, \mathbf{Z})$ action on the boundary T^2 is implemented on the Hilbert space using the operators S and T which form a representation of the $SL(2, \mathbf{Z})$,

$$S^2 = (ST)^3 = C, \quad \text{where } C_{R_1, R_2} = \delta_{\bar{R}_1, R_2}. \quad (10)$$

In the basis chosen above the T operator is diagonal with eigenvalue $e^{2\pi i(h_R - c/24)}$ when acting on the state $|R\rangle$. The S operator is not diagonal and is given by

$$S_{R_1, R_2} := K \sum_{w \in W} \epsilon(w) e^{-\frac{2\pi i}{k+N}(w(\lambda_{R_1+\rho}, \lambda_{R_2+\rho})}. \quad (11)$$

Where K only depends on k and N and W is the Weyl group. From the relation between the Hilbert space of the Chern-Simons theory and the space of conformal blocks of the WZW theory [34] it follows that the matrix element $W_{R_1, R_2} := \langle \bar{R}_1 | S^{-1} | R_2 \rangle$ is the link invariant associated with the Hopf link of linking number $+1$ [21]. This essentially follows from the path integral representation of the matrix element in the Chern-Simons theory. Since the action of T is diagonal it follows that [21]

$$\langle \bar{R}_1 | T^m S^{-1} T^n | R_2 \rangle = \langle \bar{R}_1 | S^{-1} | R_2 \rangle (-1)^{ml_{R_1} + nl_{R_2}} q^{\frac{1}{2}(m\kappa_{R_2} + n\kappa_{R_1})}, \quad (12)$$

where l_R as defined before is the number of boxes in the Young-Tableaux of representation R and $q = e^{\frac{2\pi i}{k+N}}$. The integers κ_R are defined in terms of the number of rows $d(\mu^R)$ in the Young Tableaux μ^R and number of boxes in a given row μ_i^R as

$$\kappa_R = l_R + \sum_{i=1}^{d(\mu^R)} \mu_i^R (\mu_i^R - 2i). \quad (13)$$

Thus we only need to calculate the matrix elements of S^{-1} which can be done easily using the results of [35, 36, 21] as we will explain now.

W_{R_1, R_2} : The matrix element is a function of q and $\lambda := q^N$. It is defined using the following q -numbers,

$$[x] := q^{\frac{x}{2}} - q^{-\frac{x}{2}}, \quad [x]_\lambda = \lambda^{\frac{1}{2}} q^{\frac{x}{2}} - \lambda^{-\frac{1}{2}} q^{\frac{x}{2}}, \quad (14)$$

and a polynomial associated with each Young-Tableaux μ^R given by

$$s_{\mu^R}(P(t)) = \det_{i,j} e_{\widehat{\mu}_i^R + j - i}, \quad e_0 = 1, \quad e_{k < 0} = 0. \quad (15)$$

Where $\widehat{\mu}^R$ is the Young-Tableaux obtained by interchanging the rows and the columns and e_i are such that $P(t) = 1 + \sum_{n=1}^{\infty} e_n t^n$. For example,

$$\begin{aligned} s_{\square} &= e_1, \quad s_{\blacksquare} = e_1^2 - e_2, \quad s_{\blacksquare} = e_2, \\ s_{\square\square} &= e_3 - 2e_1e_2 + e_1^3, \quad s_{\blacksquare} = e_3, \quad s_{\blacksquare} = e_3 - e_1e_2. \end{aligned} \quad (16)$$

The matrix element W_{R_1, R_2} is given by [35, 36, 21]

$$W_{R_1, R_2} := \dim_q R_1 (\lambda q)^{\frac{l_{R_2}}{2}} s_{\mu^{R_2}}(E_{\mu^{R_1}}(t)). \quad (17)$$

Where

$$\dim_q R := \prod_{1 \leq i < j \leq d(\mu^R)} \frac{[\mu_i - \mu_j + j - i]}{[j - i]} \prod_{i=1}^{d(\mu^R)} \frac{\prod_{v=-i+1}^{\mu_i-i} [v]_\lambda}{\prod_{v=1}^{\mu_i} [v - i + d(\mu^R)]}. \quad (18)$$

and

$$E_{\mu^R}(t) = \left(\prod_{j=1}^{d(\mu^R)} \frac{1 + q^{\mu_j - j} t}{1 + q^{-j} t} \right) \left(1 + \sum_{n=1}^{\infty} \left(\prod_{i=1}^n \frac{1 - \lambda^{-1} q^{i-1}}{q^i - 1} \right) t^n \right). \quad (19)$$

We will see later that in the large N limit keeping q fixed we will only need the leading order term, coefficient of $\lambda^{\frac{l_{R_1} + l_{R_2}}{2}}$, in W_{R_1, R_2} which we denote by \mathcal{W}_{R_1, R_2} . It is easy to calculate the leading order term since the expression for $E_0(t)$ simplifies in this limit and because the leading order term in $\dim_q R$ can be explicitly calculated and is given by [21]

$$q^{\kappa_{R/4}} \prod_{1 \leq i < j \leq d(\mu^R)} \frac{[\mu_i - \mu_j + j - i]}{[j - i]} \prod_{i=1}^{d(R)} \prod_{v=1}^{\mu_i} \frac{1}{[v - i + d(\mu^R)]}. \quad (20)$$

We list here \mathcal{W}_{R_1, R_2} for a few representations which we will need later for computing integer invariants.

$$\begin{aligned} \mathcal{W}_{\underbrace{\square \square \dots \square}_n} &= \frac{q^{n(n-1)/4}}{\prod_{k=1}^n (q^{k/2} - q^{-k/2})}, \\ \mathcal{W}_{A_n} &= \frac{q^{-n(n-1)/4}}{\prod_{k=1}^n (q^{k/2} - q^{-k/2})}, \\ \mathcal{W}_{\square, \square} &= \frac{((q + q^{-1} - 1))}{(q^{1/2} - q^{-1/2})^2}, \\ \mathcal{W}_{\square \square, \square} &= \frac{1}{(q^{1/2} - q^{-1/2})^3} \frac{(1 - q^2 + q^3)}{1 + q}, \\ \mathcal{W}_{\square \square, \square} &= \frac{1}{(q^{1/2} - q^{-1/2})^3} \frac{q^{-2}(1 - q + q^3)}{1 + q}, \\ \mathcal{W}_{\square \square \square, \square} &= \frac{1}{(q^{1/2} - q^{-1/2})^4} \frac{q^2(1 - q^3 + q^4)}{(1 + q)(1 + q + q^2)}, \\ \mathcal{W}_{\square \square \square, \square} &= \frac{1}{(q^{1/2} - q^{-1/2})^4} \frac{1 - q + q^2 - q^3 + q^4}{1 + q + q^2}, \end{aligned} \quad (21)$$

$$\begin{aligned}
\mathcal{W}_{\begin{array}{|c|} \hline \square \\ \hline \square \\ \hline \end{array}, \begin{array}{|c|} \hline \square \\ \hline \end{array}} &= \frac{1}{(q^{1/2} - q^{-1/2})^4} \frac{q^{1/2}(1 - q + q^4)}{(1 + q)(1 + q + q^2)} \\
\mathcal{W}_{\begin{array}{|c|} \hline \square \\ \hline \square \\ \hline \end{array}, \begin{array}{|c|} \hline \square \\ \hline \square \\ \hline \end{array}} &= \frac{1}{(q^{1/2} - q^{-1/2})^4} \frac{q^{1/2}}{1 + q}, \\
\mathcal{W}_{\begin{array}{|c|} \hline \square \\ \hline \square \\ \hline \end{array}, \begin{array}{|c|} \hline \square \\ \hline \square \\ \hline \end{array}} &= \frac{1}{(q^{1/2} - q^{-1/2})^4} \frac{q^{-1}(1 - q^2 + q^4)}{(1 + q)^2}, \\
\mathcal{W}_{\begin{array}{|c|} \hline \square \\ \hline \square \\ \hline \end{array}, \begin{array}{|c|} \hline \square \\ \hline \square \\ \hline \end{array}} &= \frac{1}{(q^{1/2} - q^{-1/2})^4} \frac{q^{-4}(1 - q + q^2 + 2q^3 - q^5 + q^6)}{(1 + q)^2}.
\end{aligned}$$

Where A_n is the Young-Tableaux with a single column of n rows and $\mathcal{W}_{R_1} = \mathcal{W}_{R_1, 0}$.

4 Resolved Conifold

We begin by considering the case of the resolved conifold with the following web diagram. The operator at the right left vertex is S^{-1} which takes $\begin{pmatrix} 0 \\ 1 \end{pmatrix}$ to $\begin{pmatrix} 1 \\ 0 \end{pmatrix}$ and the operator at the right vertex is also S^{-1} since it takes $\begin{pmatrix} 0 \\ -1 \end{pmatrix}$ to $\begin{pmatrix} -1 \\ 0 \end{pmatrix}$. With vacuum states associated with the boundary circles at infinity we get the amplitude

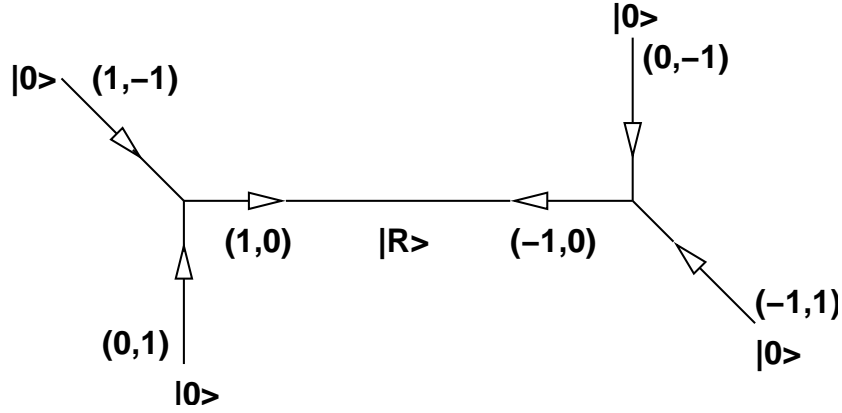


Figure 7: 5-brane web of the resolved conifold with vacuum states associated to the boundary circles.

$$\begin{aligned}
Z_{conifold} &= \sum_R \langle 0, 0 | S^{-1} | R \rangle e^{-l_R r} \langle \bar{R} | S^{-1} | 0, 0 \rangle, \\
&= \sum_R \langle 0 | S^{-1} | R \rangle e^{-l_R r} \langle \bar{R} | S^{-1} | 0 \rangle.
\end{aligned} \tag{22}$$

We claim that the instanton corrections to the topological closed string amplitude on the resolved conifold $F_{inst}^{(c)}$ is given by

$$F_{inst}^{(c)}(T) = -\log Z_{conifold}(r), \quad q = e^{igs}. \quad (23)$$

Where T is the renormalized Kähler parameter. Thus $-\log Z_{conifold}$ gives the instanton corrections to the closed topological string amplitude when written in terms of the renormalized Kähler parameter T . To determine the relation between r and T we calculate the term proportional to e^{-r} ,

$$\begin{aligned} I_1 &= e^{-r} \langle 0|S^{-1}|R\rangle \langle \bar{R}|S^{-1}|0\rangle, \\ &= e^{-r} W_{\square}^2, \\ &= e^{-r} \left(\frac{\lambda^{1/2} - \lambda^{-1/2}}{q^{1/2} - q^{-1/2}} \right)^2. \end{aligned} \quad (24)$$

In the large N limit $\lambda \mapsto \infty$ and therefore to get a finite non-vanishing result we define T as follows

$$r = T + \log(\lambda). \quad (25)$$

Then we can write Eq(23) as

$$e^{-F_{inst}^{(c)}} = \sum_R e^{-l_R T} \mathcal{W}_R^2(q). \quad (26)$$

Where as defined in the last section before $\mathcal{W}_R(q)$ is the coefficient of $\lambda^{l_R/2}$ in $W_R(q) := \langle 0|S^{-1}|R\rangle$. To see this gives the correct closed string expansion we calculate a few terms. Denoting the term proportional to e^{-nT} by I_n we have,

$$\begin{aligned} I_1 &:= e^{-T} \mathcal{W}_{\square}^2 = e^{-T} \frac{1}{(q^{1/2} - q^{-1/2})^2} \\ I_2 &:= e^{-2T} \{ \mathcal{W}_{\square\square}^2 + \mathcal{W}_{\square}^2 \} = e^{-2T} \frac{q + q^{-1}}{(q^{1/2} - q^{-1/2})^4 (q^{1/2} + q^{-1/2})^2}, \\ I_3 &:= e^{-3T} \{ \mathcal{W}_{\square\square\square}^2 + \mathcal{W}_{\square\square}^2 + \mathcal{W}_{\square}^2 \} = e^{-3T} \frac{(q^3 + q^{-3}) + (q + q^{-1}) + 2}{(q^{1/2} - q^{-1/2})^4 (q^{1/2} + q^{-1/2})^2 (q^{3/2} - q^{-3/2})^2}, \\ I_4 &:= e^{-4T} \{ \mathcal{W}_{\square\square\square\square}^2 + \mathcal{W}_{\square\square\square}^2 + \mathcal{W}_{\square\square}^2 + \mathcal{W}_{\square}^2 + \mathcal{W}_{\square}^2 \} \\ &= e^{-4T} \frac{C(q)}{(q^{1/2} - q^{-1/2})^6 (q^{1/2} + q^{-1/2})^4 (q + q^{-1})^2 (q^{3/2} - q^{-3/2})^2}. \end{aligned} \quad (27)$$

Where

$$C(q) := (q^6 + q^{-6}) + (q^4 + q^{-4}) + 2(q^3 + q^{-3}) + 4(q^2 + q^{-2}) + 2(q + q^{-1}) + 4. \quad (28)$$

Since the resolved conifold has a single \mathbb{P}^1 from Eq(1) it follows that the closed string expansion for the conifold is given by [10]

$$F_{inst}^{(c)}(T) = \sum_{n=1}^{\infty} \sum_{g=0}^{\infty} \frac{N_C^g}{n} (2\sin(n g_s/2))^{2g-2} e^{-nT} . \quad (29)$$

Comparing this with Eq(26) using Eq(27) we get

$$\begin{aligned} -\log Z_{conifold} &= \log(1 + I_1 + I_2 + I_3 + I_4 + \dots), \quad (30) \\ &= I_1 + \left\{ I_2 - \frac{1}{2} I_1^2 \right\} + \left\{ I_3 - I_2 I_1 + \frac{1}{3} I_1^3 \right\} + \left\{ I_4 - I_3 I_1 + I_2 I_1^2 - \frac{1}{2} I_2^2 - \frac{1}{4} I_1^4 \right\} + \dots, \\ &= \frac{e^{-T}}{(2\sin(g_s/2))^2} + \frac{e^{-2T}}{2(2\sin(g_s))^2} + \frac{e^{-3T}}{3(2\sin(3g_s/2))^2} + \frac{e^{-4T}}{4(2\sin(2g_s))^2} + \dots \end{aligned}$$

Which agrees with the expected closed string expansion.

5 Calabi-Yau with single compact divisor

In this section we will discuss non-compact toric Calabi-Yau threefolds which have a single compact divisor. These Calabi-Yau manifolds are the total space of the canonical line bundle over a toric Fano or toric almost Fano surface. We will consider the case of blowups of \mathbb{P}^2 and the blowups of first and second Hirzebruch surfaces. We denote the blow up of \mathbb{P}^2 at k points by \mathcal{B}_k .

5.1 \mathbb{P}^2

The amplitude associated with the web diagram can be written down completely once the gluing matrices associated with each vertex are known. All Riemann surfaces corresponding to the 5-brane webs can be constructed from a "propagator" (a cylinder) and $SL(2, \mathbf{Z})$ transform of a "three point vertex" (a sphere with three disks removed). The $SL(2, \mathbf{Z})$ gluing matrices associated with the vertices of the brane web contain the information about how the propagators and the three point vertex are to be put together to get the web. These gluing matrices are $SL(2, \mathbf{Z})$ matrices which transform one edge of the three point vertex with charge (p, q) into another edge with charge (r, s) . For the case of non-compact Calabi-Yaus with a single compact divisor the Riemann surface is of genus one which is reflected by the fact that the 5-brane web has a single "face". In this case we see that each three point vertex used to construct the web has two edges which are the internal edges and therefore it is natural to define the gluing matrix at that vertex to be the $SL(2, \mathbf{Z})$ matrix which maps

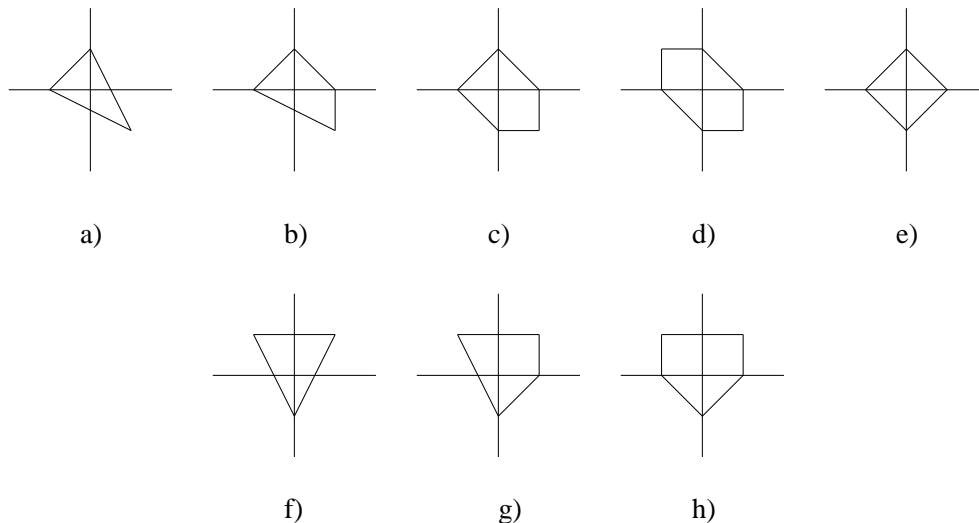


Figure 8: a) \mathbb{P}^2 , b) \mathcal{B}_1 , c) \mathcal{B}_2 , d) \mathcal{B}_3 , e) $\mathbb{P}^1 \times \mathbb{P}^1$, f) F_2 , g) F_2 blown up at one point, h) F_2 blown up at two points.

one internal edge to another internal edge associated with that vertex consistent with the vertex defined before.

We begin with the case of \mathbb{P}^2 , which was discussed in detail in [21], for completeness. The non-compact Calabi-Yau manifold is the total space of $\mathcal{O}(-3)$ bundle over \mathbb{P}^2 . The web diagram dual to this non-compact CY can be obtained from the toric diagrams given in Fig. 8(a) and is shown in Fig. 9. The equation for the Riemann surface which gives the dual theory when M5-brane is wrapped on it can be easily determined from the mirror superpotential or the toric data [29, 30]

$$1 + e^u + e^v + e^{-t-u-v} = 0. \quad (31)$$

Where t is the Kähler parameter of the generator of $H_2(\mathbb{P}^2, \mathbf{Z})$ which we will denote by H . H is the class of \mathbb{P}^1 given by a linear equation in \mathbb{P}^2 and is such that $H \cdot H = 1$. From the web diagram we can determine the operators associated with the vertices. These operators are just the operators in the WZW theory corresponding to the $SL(2, \mathbf{Z})$ matrices mapping the internal edges into each other at each vertex,

$$\begin{pmatrix} 0 \\ 1 \end{pmatrix} \xrightarrow{\mathcal{V}_1} \begin{pmatrix} 1 \\ 0 \end{pmatrix} \xrightarrow{\mathcal{V}_2} \begin{pmatrix} -1 \\ -1 \end{pmatrix} \xrightarrow{\mathcal{V}_3} \begin{pmatrix} 0 \\ 1 \end{pmatrix}, \quad (32)$$

$$\mathcal{V}_1 = S^{-1}, \quad \mathcal{V}_2 = TS^{-1}T, \quad \mathcal{V}_3 = TS^{-1}.$$

Given these operators associated with the vertices we can write down the instanton contribution to the closed string amplitude (this can also be obtained as the large N limit of the

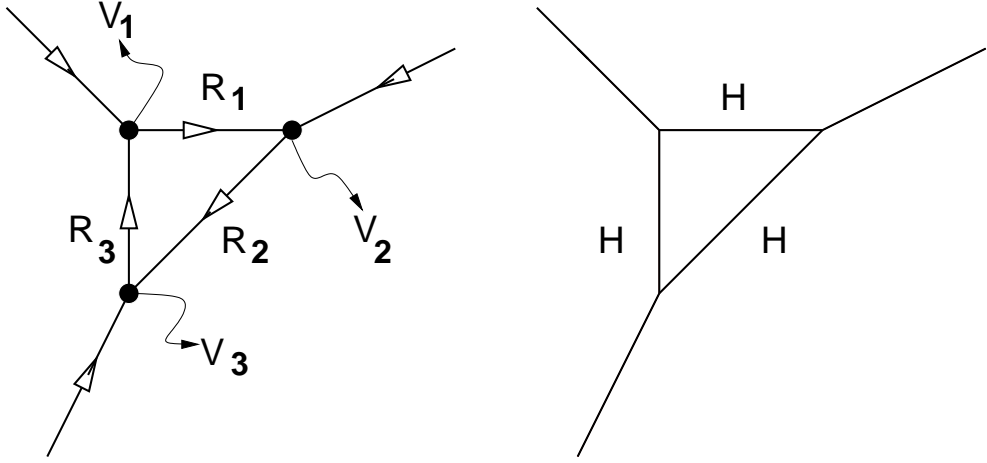


Figure 9: a) The 5-brane web dual to the local \mathbb{P}^2 , (p, q) 5-brane is oriented in the direction (p, q) . R_a denote the states propagating on the internal lines, b) the rational curve classes of the internal edges.

Chern-Simons theory on local B_3 with three non intersecting exceptional curves geometrically transitioned to S^3 as was done in [21]),

$$\begin{aligned}
e^{F_{inst}^{(c)}} &= \sum_{R_1, R_2, R_3} e^{-\sum_{a=1}^3 l_a r_a} \langle \bar{R}_3 | \mathcal{V}_3 | R_2, 0 \rangle \langle \bar{R}_2 | \mathcal{V}_2 | R_1, 0 \rangle \langle \bar{R}_1 | \mathcal{V}_1 | R_3, 0 \rangle, \\
&= \sum_{R_1, R_2, R_3} e^{-\sum_{a=1}^3 l_a r_a} \langle \bar{R}_3 | \mathcal{V}_3 | R_2 \rangle \langle \bar{R}_2 | \mathcal{V}_2 | R_1 \rangle \langle \bar{R}_1 | \mathcal{V}_1 | R_3 \rangle.
\end{aligned} \tag{33}$$

Note: Local \mathbb{P}^2 blown up at more than three points have web diagrams in which some of the external legs are either parallel or cross each other. This is due to the fact that \mathbb{P}^2 blown up at more than three points is not toric although we can choose special points and blow them up. The problem of intersecting external legs was solved in [24] by placing appropriate (p, q) 7-brane and allowing the 5-brane to end on these 7-brane so that the external 5-brane no longer can go to infinity and cross each other. This 5-brane/7-brane picture can be simplified so that the web is given by a single 5-brane going around the 7-brane as shown in Fig. 10 below.

In this picture it is easy to generalize and write amplitudes for non-toric local Calabi-Yau,

$$e^{F_{inst}^{(c)}} := \sum_{a=1}^N \sum_{R_a} e^{-\sum_{i=1}^N l_i r_i} \prod_{i=1}^N \langle R_{i+1} | \mathcal{V}_{i+1} | R_i \rangle. \tag{34}$$

Where \mathcal{V}_i are the $SL(2, \mathbf{Z})$ monodromy matrices associated with the 7-branes. These amplitudes for non-toric Calabi-Yau spaces will be discussed elsewhere [18].

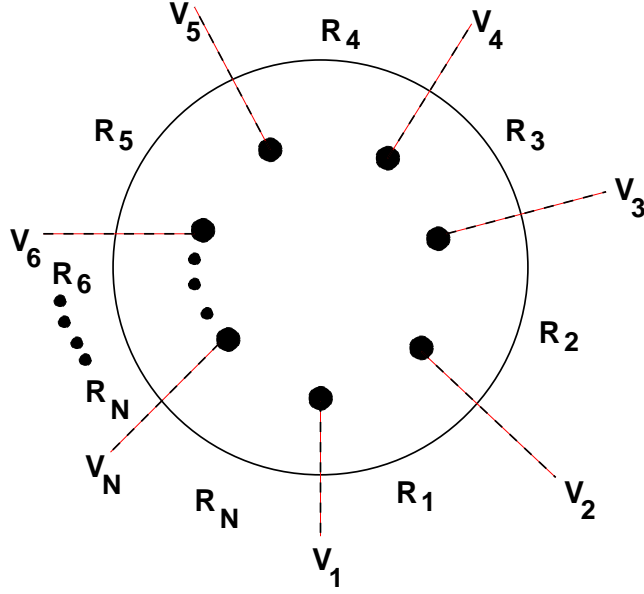


Figure 10: 5-brane/7-brane description of toric and non-toric local Calabi-Yau's.

Coming back to the local \mathbb{P}^2 case we determine the relation between r_a and the renormalized Kähler parameter by calculating the terms with only one non-vanishing l_a .

$l_a = \delta_{ab}$: We denote the term with $l_a = \delta_{ab}$ by \mathcal{I}_b ,

$$\begin{aligned}
\mathcal{I}_b &= e^{-r_b} (-1) W_{\cdot, \square}^2(\lambda, q), \\
&= -e^{-r_b} \left(\frac{\lambda^{1/2} - \lambda^{-1/2}}{q^{1/2} - q^{-1/2}} \right)^2, \\
&= \frac{e^{-T_b}}{(q^{1/2} - q^{-1/2})^2}, \\
&= \frac{e^{-T_b}}{(2\sin(g_s/2))^2}.
\end{aligned} \tag{35}$$

Where the minus sign comes from the action of T operator on the state with fundamental representation $|\square\rangle$ and we have defined $r_b = T_b + \log(\lambda)$ before taking the limit $\lambda \mapsto \infty$. T_b is the "renormalized Kähler parameter of the rational curve which lives on the b -th internal edge of the web diagram. Since all the rational curves living on the internal edge of the web diagram are in the same class H therefore we can set $T_1 = T_2 = T_3 =: T_H$. After this redefinition we see that we only need the leading order terms in λ in the matrix elements $\langle \bar{R} | S^{-1} | \bar{R}' \rangle$ as noted in [21],

$$e^{F_{inst}^{(c)}} = \sum_{R_1, R_2, R_3} e^{-(l_1 + l_2 + l_3)(T_H - i\pi)} \mathcal{W}_{R_3, R_2} \mathcal{W}_{R_2, R_1} \mathcal{W}_{R_1, R_3} q^{\frac{1}{2}(\kappa_{R_1} + \kappa_{R_2} + \kappa_{R_3})}. \tag{36}$$

5.1.1 Integer invariants of few curve classes

We evaluate the invariants for the curve classes $H, 2H$ and $3H$. Terms contribution to nH are proportional to e^{-nT_H} and therefore $l_1 + l_2 + l_3 = n$. For $n = 1$ it follows from Eq(36) that

$$\mathcal{I}(H) = -3e^{-T_H} \mathcal{W}_{\square}^2. \quad (37)$$

For $n = 2$ we have from Eq(36),

$$\mathcal{I}(2H) = e^{-2T_H} (3q\mathcal{W}_{\square\square}^2 + 3q^{-1}\mathcal{W}_{\square}^2 + 3\mathcal{W}_{\square}^2 \mathcal{W}_{\square,\square}), \quad (38)$$

$$= e^{-2T_H} 3q^{-1} (2(q^2 + q^{-2}) + (q + q^{-1})) \text{cal} \mathcal{W}_{\square}^2. \quad (39)$$

For $n = 3$,

$$\begin{aligned} \mathcal{I}(3H) &= -e^{-3T_H} (3q^3\mathcal{W}_{\square\square\square}^2 + 3q^{-3}\mathcal{W}_{\square}^2 + 3\mathcal{W}_{\square}^2 + \\ &\quad 6q\mathcal{W}_{\square}\mathcal{W}_{\square\square}\mathcal{W}_{\square,\square} + 6q^{-1}\mathcal{W}_{\square}\mathcal{W}_{\square}\mathcal{W}_{\square,\square} + \mathcal{W}_{\square,\square}^2) \\ &= -e^{-3T_H} q^{-3} P(q) \mathcal{W}_{\square\square\square}^2, \\ P(q) &:= 10(q^6 + q^{-6}) + 7(q^5 + q^{-5}) + 8(q^4 + q^{-4}) + 3(q^3 + q^{-3}) \\ &\quad + 10(q^2 + q^{-2}) + 26(q + q^{-1}) + 34 \end{aligned}$$

Thus up to e^{-3T} the closed string expansion is given by

$$\begin{aligned} F_{inst}^{(c)} &= \log(1 + \mathcal{I}(H) + \mathcal{I}(2H) + \mathcal{I}(3H) + \dots) \quad (40) \\ &= \mathcal{I}(H) + \{\mathcal{I}(2H) - \frac{1}{2}\mathcal{I}(H)^2\} + \{\mathcal{I}(3H) - \mathcal{I}(H)\mathcal{I}(2H) + \frac{1}{3}\mathcal{I}(H)^3\} + \dots, \\ &= e^{-T_H} \frac{3}{(2\sin(g_s/2))^2} + e^{-2T_H} \left\{ \frac{3}{2(2\sin(g_s))^2} - \frac{6}{(2\sin(g_s/2))^2} \right\} + e^{-3T_H} \left\{ \frac{3}{3(\sin(3g_s/2))^2} \right. \\ &\quad \left. + \frac{27}{(2\sin(g_s/2))^2} - 10 \right\} + \dots \end{aligned}$$

To get the integer invariant we compare the above expansion with the close string expansion

$$\begin{aligned} F_{inst}^{(c)} &= e^{-T_H} \frac{N_H^0}{(2\sin(g_s/2))^2} + e^{-2T_H} \left\{ \frac{N_H^0}{2(2\sin(g_s))^2} + \frac{N_{2H}^0}{(2\sin(g_s/2))^2} \right\} + e^{-3T_H} \left\{ \frac{N_H^0}{3(\sin(3g_s/2))^2} \right. \\ &\quad \left. + \frac{N_{3H}^0}{(2\sin(g_s/2))^2} + N_{3H}^1 \right\} + \dots, \end{aligned}$$

to obtain $N_H^g = 3\delta_{g,0}$, $N_{2H}^g = -6\delta_{g,0}$ and $N_{3H}^g = 27\delta_{g,0} - 10\delta_{g,1}$.

5.2 local \mathcal{B}_1

Consider now the case of a non-compact Calabi-Yau with a compact divisor which is \mathbb{P}^2 blown up at one point, \mathcal{B}_1 . The case when the divisor is a \mathbb{P}^2 can also be obtained from this as we will show later. We will see that the geometry of the web (or the Riemann surface given by mirror symmetry) when interpreted as a Feynman diagram completely determines instanton corrections to the closed topological string amplitude.

The geometry of the web corresponding to local \mathcal{B}_1 is shown in Fig. 11. The Riemann surface

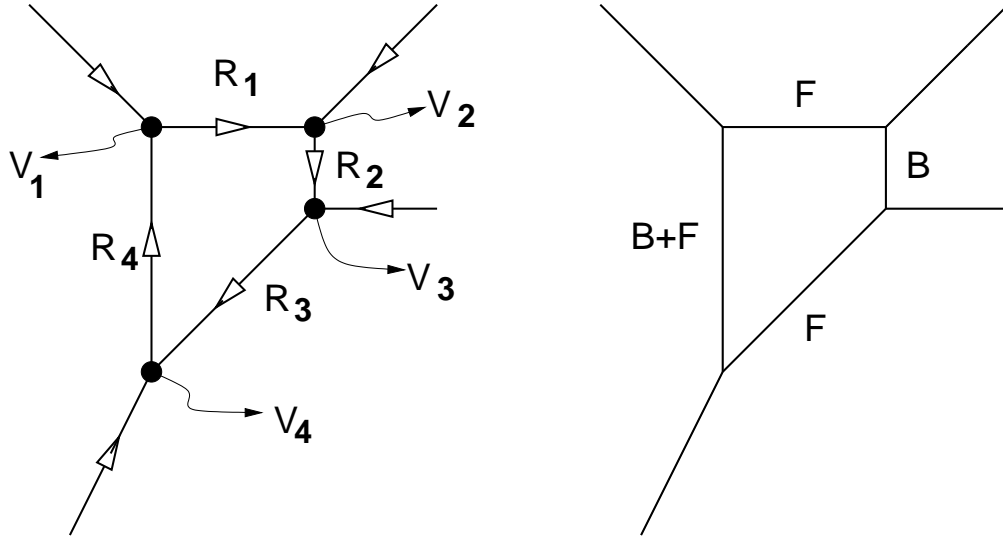


Figure 11: The 5-brane web dual to the local \mathcal{B}_1 , b) rational curves associated with the internal edges.

can be obtained by thickening the web and is given by the following equation,

$$1 + e^u + e^v + e^{-t_1 - u + v} + e^{-t_2 - u} = 0. \quad (41)$$

This equation as well as the 5-brane web can be easily obtained from the toric data shown in Fig. 8.

5.2.1 Kähler parameters and homology

\mathcal{B}_1 is \mathbb{P}^2 blown up at one point and therefore has $\dim H_2(\mathcal{B}_1) = 2$. As a basis we take the curves given by $B := E$ and $F := H - E$ where H is the class coming from \mathbb{P}^2 and E is the class of the exceptional curve obtained by blowing up. The intersection matrix is then ,

$$B^2 = -1, \quad B \cdot F = 1, \quad F^2 = 0. \quad (42)$$

We have used the fact that \mathcal{B}_1 is a \mathbb{P}^1 bundle over \mathbb{P}^1 to use as basis the base \mathbb{P}^1 and the fiber \mathbb{P}^1 denoted by B and F respectively. We denote by $t_{B,F}$ the Kähler parameters of B and F . Since intersection numbers between effective curves must be non-negative it follows that for $nB + mF$ to be effective and therefore contribute to the topological string amplitudes we must have

$$(nB + mF) \cdot B \geq 0 \mapsto m \geq n \text{ if } m \neq 0 \quad (43)$$

Each internal line of the web corresponds to a curve in \mathcal{B}_1 . Denoting these curves by C_a it follows that these curves are not independent ($-K_{\mathcal{B}_1}$ is the class dual to the first Chern class of \mathcal{B}_1)

$$\sum_{a=1}^4 C_a = -K_{\mathcal{B}_1} = 2B + 3F. \quad (44)$$

It follows that

$$C_1 = F, C_2 = B, C_3 = F, C_4 = B + F. \quad (45)$$

From the web diagram, Fig. 11, it is easy to write down the gluing matrices \mathcal{V}_a associated with the vertices,

$$\begin{aligned} & \begin{pmatrix} 0 \\ 1 \end{pmatrix} \xrightarrow{\mathcal{V}_1} \begin{pmatrix} 1 \\ 0 \end{pmatrix} \xrightarrow{\mathcal{V}_2} \begin{pmatrix} 0 \\ -1 \end{pmatrix} \xrightarrow{\mathcal{V}_3} \begin{pmatrix} -1 \\ -1 \end{pmatrix} \xrightarrow{\mathcal{V}_4} \begin{pmatrix} 0 \\ 1 \end{pmatrix}, \\ & \mathcal{V}_1 = S^{-1}, \mathcal{V}_2 = S^{-1}, \mathcal{V}_3 = S^{-1}T^{-1}, \mathcal{V}_4 = TS^{-1}. \end{aligned} \quad (46)$$

The amplitude associated with the above 5-brane web is obtained by interpreting the corresponding Riemann surface/web as a one loop Feynman diagram with four external states. We take the states associated with the external legs to be vacuum states $|0\rangle$. And the states $|R_a\rangle$ propagating in the loop are summed over. With this prescription the amplitude whose log gives the topological closed string instanton corrections is given by

$$\begin{aligned} e^{F_{inst}^{(c)}} & := \sum_{R_1, R_2, R_3, R_4} e^{-\sum_{a=1}^4 l_{R_a} r_a} \langle \bar{R}_4 | \mathcal{V}_4 | R_3, 0 \rangle \langle \bar{R}_3 | \mathcal{V}_3 | R_2, 0 \rangle \langle \bar{R}_2 | \mathcal{V}_2 | R_1, 0 \rangle \langle \bar{R}_1 | \mathcal{V}_1 | 0, R_4 \rangle. \\ & = \sum_{R_1, R_2, R_3, R_4} e^{-\sum_{a=1}^4 l_{R_a} r_a} \langle \bar{R}_4 | \mathcal{V}_4 | R_3 \rangle \langle \bar{R}_3 | \mathcal{V}_3 | R_2 \rangle \langle \bar{R}_2 | \mathcal{V}_2 | R_1 \rangle \langle \bar{R}_1 | \mathcal{V}_1 | R_4 \rangle. \end{aligned}$$

In the above equation r_a is the length of the internal edge, l_a is the number of boxes in the Young Tableau corresponding to the representation R_a and the term $e^{-l_a r_a}$ comes from the propagator joining the states at two adjacent vertices. Note that not all r_a are actually independent as we will see below. Note that if $r_2 = 0$ we can sum over R_2 and obtain the expression for the local \mathbb{P}^2 case [21].

To determine the relation between r_a and the renormalized Kähler parameters $T_{B,F}$ we evaluate terms in the Eq(47) with only one non-vanishing l_a .

$l_a = \delta_{ab}$: We denote this term by I_b ,

$$\begin{aligned} I_b &:= (-1)^{\delta_{b,2}+\delta_{b,4}} e^{-r_b} W_{\square}^2(q, \lambda), \\ &= (-1)^{\delta_{b,2}+\delta_{b,4}} e^{-r_b} \left(\frac{\lambda^{1/2} - \lambda^{-1/2}}{q^{1/2} - q^{-1/2}} \right)^2. \end{aligned} \quad (47)$$

In order to obtain a finite non-vanishing I_b in the limit $\lambda \mapsto \infty$ we define the renormalized Kähler parameter T_b associated with curves C_b as follows

$$T_b := r_b - \log(\lambda). \quad (48)$$

Thus from the above equation and Eq(45) we get

$$\begin{aligned} r_1 &= T_1 + \log(\lambda) = T_F + \log(\lambda), \\ r_2 &= T_2 + \log(\lambda) = T_B + \log(\lambda), \\ r_3 &= T_3 + \log(\lambda) = T_F + \log(\lambda), \\ r_4 &= T_4 + \log(\lambda) = T_B + T_F + \log(\lambda). \end{aligned} \quad (49)$$

5.2.2 Integer invariants of few curve classes

Using the above definition of r_a in terms of $T_{B,F}$ we can write Eq(47) as

$$e^{F_{inst}^{(c)}} = \sum_{a=1}^4 \sum_{R_a} e^{-l_B T_B - l_F T_F} \mathcal{W}_{R_4, R_3} \mathcal{W}_{R_3, R_2} \mathcal{W}_{R_2, R_1} \mathcal{W}_{R_1, R_4} (-1)^{l_2+l_4} q^{\frac{1}{2}(\kappa_{R_4} - \kappa_{R_2})}.$$

where

$$l_B := l_2 + l_4, \quad l_F := l_1 + l_3 + l_4, \quad (50)$$

and \mathcal{W}_{R_a, R_b} are the coefficient of the leading power of λ , $\lambda^{\frac{l_a+l_b}{2}}$, in $\langle R_a | S^{-1} | R_b \rangle$ and some of them are listed in section 3. We denote the term with $e^{-mT_F - nT_B}$ in the above expansion by $\mathcal{I}(nB + mF)$. Using Eq(50) we evaluate the integer invariants associated with B , F and $B + F$.

B : To obtain the coefficient of e^{-T_B} we see that we must have $l_1 = l_3 = l_4 = 0$ and $l_2 = 1$,

$$\begin{aligned} \mathcal{I}(B) &= -e^{-T_B} \mathcal{W}_{\square}^2, \\ &= -\frac{e^{-T_B}}{(q^{1/2} - q^{-1/2})^2}, \\ &= \frac{e^{-T_B}}{(2\sin(g_s/2))^2}, \end{aligned} \quad (51)$$

where $\lambda = q^N$ and $q = e^{igs}$. Since this curve class is not a multiple of another curve class therefore we do not have to take into account any multiple cover contributions and comparing it with the closed string expansion gives

$$N_B^0 = 1, \quad N_B^g = 0, \quad g > 0. \quad (52)$$

Which is indeed the correct result given that the exceptional curve B is rigid and has zero dimensional moduli space.

F : In this case we must have $(l_1, l_2, l_3, l_4) = (1, 0, 0, 0)$ or $(0, 0, 1, 0)$. Again denoting the term by $\mathcal{I}(F)$ we get

$$\begin{aligned} \mathcal{I}(F) &= e^{-T_F} 2 \mathcal{W}_{\square}^2, \\ &= -\frac{2 e^{-T_F}}{(2\sin(g_s/2))^2}. \end{aligned} \quad (53)$$

Again since there are no multiple cover contribution to be subtracted comparing with the closed string expansion gives

$$N_F^0 = -2, \quad N_F^g = 0 \quad g > 0. \quad (54)$$

Which is indeed the correct result, since its moduli space is just the base curve which is \mathbb{P}^1 (since F is genus zero the moduli space of flat connections is trivial) and therefore $N_F^0 = (-1)^{\dim \mathcal{M}_F} \chi(\mathcal{M}_F) = -2$.

$B + F$: Terms contributing in this case are the ones with $(l_1, l_2, l_3, l_4) = (1, 1, 0, 0), (0, 1, 1, 0)$ and $(0, 0, 0, 1)$.

$$\begin{aligned} \mathcal{I}(B + F) &= e^{-T_B - T_F} \{-2 \mathcal{W}_{\square}^2 \mathcal{W}_{\square, \square} - \mathcal{W}_{\square}^2\}, \\ &= \frac{3 e^{-T_B - T_F}}{(2\sin(g_s/2))^2} - \frac{2 e^{-T_B - T_F}}{(2\sin(g_s/2))^4}. \end{aligned} \quad (55)$$

Thus we get

$$\begin{aligned} F_{inst}^{(c)} &= \log(1 + \mathcal{I}(B) + \mathcal{I}(F) + \mathcal{I}(B + F) + \dots), \\ &= \mathcal{I}(B) + \mathcal{I}(F) + \mathcal{I}(B + F) - \mathcal{I}(B)\mathcal{I}(F) + \dots, \\ &= \frac{e^{-T_B}}{(2\sin(g_s/2))^2} - \frac{2e^{-T_F}}{(2\sin(g_s/2))^2} + \frac{3e^{-T_B - T_F}}{(2\sin(g_s/2))^2} + \dots \end{aligned} \quad (56)$$

Thus we get

$$N_{B+F}^0 = 3, \quad N_{B+F}^g = 0, \quad g > 0. \quad (57)$$

Which is indeed correct since $B + F = H$.

5.3 \mathcal{B}_2

\mathcal{B}_2 is \mathbb{P}^2 blown-up at two points and can also be obtained from $\mathbb{P}^1 \times \mathbb{P}^1$ by blowing up one point. The 5-brane web diagram can be obtained from the toric diagram 8 directly or can be obtained from the mirror Riemann surface

$$1 + e^u + e^v + e^{-t_1 - u - v} + e^{-t_2 - u} + e^{-t_3 - v}, \quad (58)$$

which is embedded in $\mathbb{R}^2 \times T^2$ by taking the Kähler parameter of T^2 to zero. Both these description give the same 5-brane web shown in Fig. 12 below. From the toric diagram we

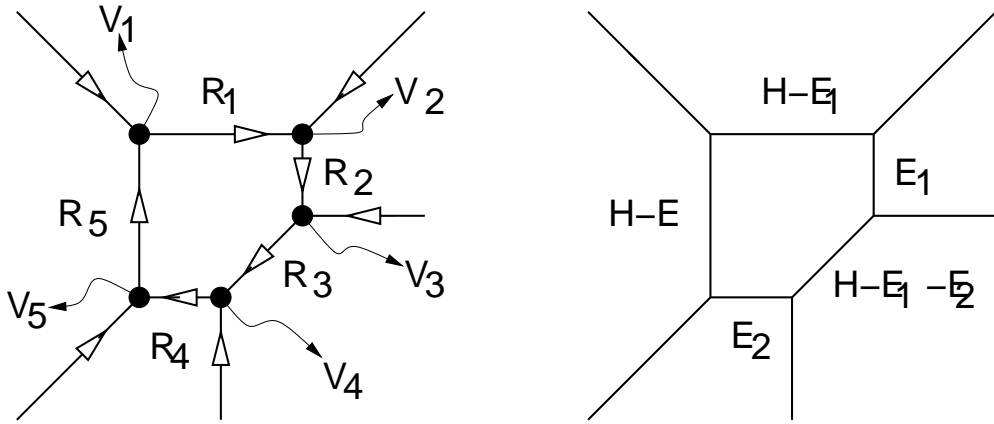


Figure 12: 5-brane web dual to local B_2 .

immediately obtain the $SL(2, \mathbf{Z})$ matrices associated with the trivalent vertices,

$$\begin{pmatrix} 0 \\ 1 \end{pmatrix} \xrightarrow{\mathcal{V}_1} \begin{pmatrix} 1 \\ 0 \end{pmatrix} \xrightarrow{\mathcal{V}_2} \begin{pmatrix} 0 \\ -1 \end{pmatrix} \xrightarrow{\mathcal{V}_3} \begin{pmatrix} -1 \\ -1 \end{pmatrix} \xrightarrow{\mathcal{V}_4} \begin{pmatrix} -1 \\ 0 \end{pmatrix} \xrightarrow{\mathcal{V}_5} \begin{pmatrix} 0 \\ 1 \end{pmatrix}, \quad (59)$$

$$\mathcal{V}_1 = S^{-1}, \mathcal{V}_2 = S^{-1}, \mathcal{V}_3 = S^{-1}T^{-1}, \mathcal{V}_4 = T^{-1}S^{-1}T^{-1}, \mathcal{V}_5 = S^{-1}.$$

Using these matrices we can immediately write down the amplitude associated with the web diagram,

$$e^{F_{inst}^{(c)}} := \sum_{a=1}^5 \sum_{R_a} e^{-\sum_{b=1}^5 l_b r_b} \prod_{i=1}^5 \langle R_{i+1} | \mathcal{V}_{i+1} | R_i \rangle, \quad (60)$$

where $R_6 = R_1$ and $\mathcal{V}_6 = \mathcal{V}_1$. r_b are the bare Kähler parameters associated with the curve classes C_b forming the internal line of the web,

$$C_1 = H - E_1, C_2 = E_1, C_3 = H - E_1 - E_2, C_4 = E_2, C_5 = H - E_2. \quad (61)$$

To determine the relation between r_b and the renormalized parameters associated with C_b denoted by T_b we calculate the terms in Eq(60) with $l_a = \delta_{ab}$.

$l_a = \delta_{ab}$: we denote this term by I_b ,

$$\begin{aligned} I_b &= (-1)^{\delta_{b,2}+\delta_{b,3}+\delta_{b,4}} e^{-r_b} W_{\square}^2, \\ &= (-1)^{\delta_{b,2}+\delta_{b,3}+\delta_{b,4}} e^{-r_b} \left(\frac{\lambda^{1/2} - \lambda^{-1/2}}{q^{1/2} - q^{-1/2}} \right)^2. \end{aligned} \quad (62)$$

Thus to be able to take the limit $\lambda \mapsto \infty$ we define the r_b in terms of the renormalized Kähler parameters T_H, T_{E_1} and T_{E_2} ,

$$\begin{aligned} r_1 &= T_1 + \log(\lambda) = T_H - T_{E_1} + \log(\lambda), \\ r_2 &= T_2 + \log(\lambda) = T_{E_1} + \log(\lambda), \\ r_3 &= T_3 + \log(\lambda) = T_H - T_{E_1} - T_{E_2} + \log(\lambda), \\ r_4 &= T_4 + \log(\lambda) = T_{E_2} + \log(\lambda), \\ r_5 &= T_5 + \log(\lambda) = T_H - T_{E_2} + \log(\lambda) \end{aligned} \quad (63)$$

5.3.1 Integer invariants of few curve classes

Using the above definition of T_{H,E_1,E_2} we can write the amplitude Eq(60) as

$$e^{F_{inst}^{(c)}} = \sum_{a=1}^5 \sum_{R_a} e^{-(l_H T_H - l_{E_1} T_{E_1} - l_{E_2} T_{E_2})} (-1)^{l_2+l_3+l_4} q^{-\frac{1}{2}(\kappa_{R_2}+\kappa_{R_3}+\kappa_{R_4})} \prod_{i=1}^5 \mathcal{W}_{R_{i+1}, R_i}. \quad (64)$$

where

$$l_H = l_1 + l_3 + l_5, \quad l_{E_1} = l_1 + l_3 - l_2, \quad l_{E_2} = l_3 + l_5 - l_4. \quad (65)$$

we start with determining the invariants associated with the exceptional curves E_1, E_2 and $H - E_1 - E_2$.

E_1 : This term, which we will denote by $\mathcal{I}(E_1)$, is given by $(l_1, l_2, l_3, l_4, l_5) = (0, 1, 0, 0, 0)$,

$$\begin{aligned} \mathcal{I}(E_1) &= -e^{-T_{E_1}} \mathcal{W}_{\square}^2, \\ &= \frac{e^{-T_{E_1}}}{(2\sin(g_s/2))^2}. \end{aligned} \quad (66)$$

This implies that

$$N_{E_1}^0 = 1, \quad N_{E_1}^g = 0, \quad g > 0. \quad (67)$$

Similarly the term corresponding to E_2 is the same as above giving $N_{E_2}^0 = 1$ and $N_{E_2}^g$ for $g > 0$ as expected since the exceptional curves are rigid with zero dimensional moduli space.

$H - E_1 - E_2$ There is only term which contributes here given by $(l_1, l_2, l_3, l_4, l_5) = (0, 0, 1, 0, 0)$,

$$\begin{aligned} \mathcal{I}(H - E_1 - E_2) &= -e^{-(T_H - T_{E_1} - T_{E_2})} \mathcal{W}_{\square}^2, \\ &= \frac{e^{-T_H + T_{E_1} + T_{E_2}}}{(2\sin(g_s/2))^2}. \end{aligned} \quad (68)$$

Thus we get $N_{H-E_1-E_2}^g = \delta_{g,0}$ since $H - E_1 - E_2$ is an exceptional curve.

5.4 \mathcal{B}_3

The web diagram in this case is given by Fig. 13. The $SL(2, \mathbf{Z})$ matrices are determined by

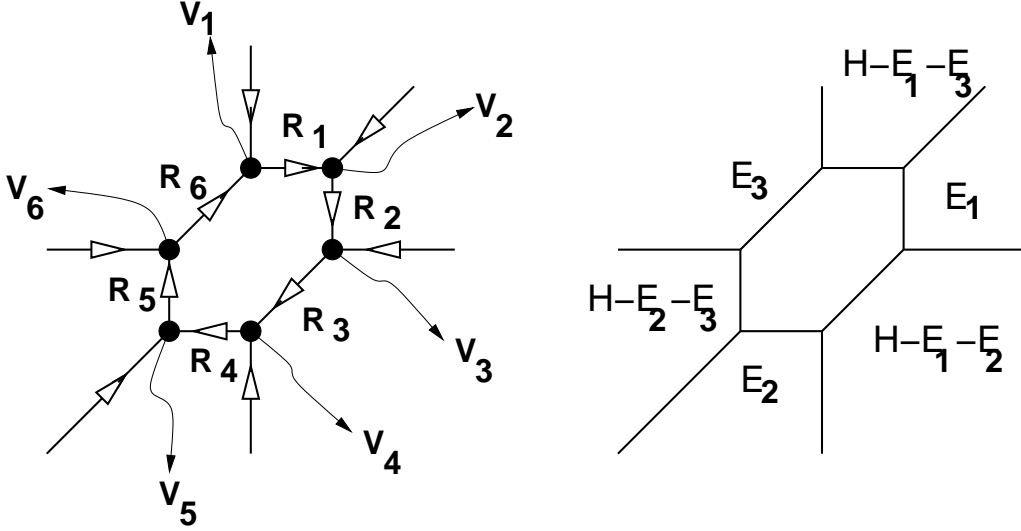


Figure 13: 5-brane web dual to local \mathcal{B}_3 .

the web diagram and are

$$\begin{aligned} \begin{pmatrix} 1 \\ 1 \end{pmatrix} \xrightarrow{\mathcal{V}_1} \begin{pmatrix} 1 \\ 0 \end{pmatrix} \xrightarrow{\mathcal{V}_2} \begin{pmatrix} 0 \\ -1 \end{pmatrix} \xrightarrow{\mathcal{V}_3} \begin{pmatrix} -1 \\ -1 \end{pmatrix} \xrightarrow{\mathcal{V}_4} \begin{pmatrix} -1 \\ 0 \end{pmatrix} \xrightarrow{\mathcal{V}_5} \begin{pmatrix} 0 \\ 1 \end{pmatrix} \xrightarrow{\mathcal{V}_6} \begin{pmatrix} 1 \\ 1 \end{pmatrix}, \\ \mathcal{V}_1 = T^{-1}S^{-1}T^{-1}, \mathcal{V}_2 = S^{-1}, \mathcal{V}_3 = S^{-1}T^{-1}, \mathcal{V}_4 = T^{-1}S^{-1}T^{-1}, \mathcal{V}_5 = S^{-1}, \mathcal{V}_6 = S^{-1}T^{-1}. \end{aligned} \quad (69)$$

Then $F_{inst}^{(c)}$ is given by

$$e^{F_{inst}^{(c)}} = \sum_{a=1}^6 \sum_{R_a} e^{-\sum_{b=1}^6 l_b r_b} \prod_{b=1}^6 \langle R_{b+1} | \mathcal{V}_{b+1} | R_b \rangle. \quad (70)$$

Where $R_7 = R_1$ and $\mathcal{V}_7 = \mathcal{V}_1$. calculation similar to the one done before gives the r_b in terms of normalized Kähler parameters $T_H, T_{E_1}, T_{E_2}, T_{E_3}$,

$$\begin{aligned}
r_1 &= T_H - T_{E_1} - T_{E_3} + \log(\lambda), \\
r_2 &= T_{E_1} + \log(\lambda), \\
r_3 &= T_H - T_{E_1} - T_{E_2} + \log(\lambda), \\
r_4 &= T_{E_2} + \log(\lambda), \\
r_5 &= T_H - T_{E_2} - T_{E_3} + \log(\lambda), \\
r_6 &= T_{E_3} + \log(\lambda).
\end{aligned} \tag{71}$$

5.4.1 Integer invariants of few curve classes

To show that this correctly reproduces the integer invariants [10] we calculate some terms in the above expansion corresponding to exceptional curves. First we rewrite Eq(70) in terms of $T_H, T_{E_1}, T_{E_2}, T_{E_3}$,

$$e^{F_{inst}^{(c)}} = \sum_{a=1}^6 \sum_{R_a} e^{-(l_H T_H - l_{E_1} T_{E_1} - l_{E_2} T_{E_2})} (-1)^{\sum_{i=1}^6 l_i} q^{-\frac{1}{2}(\sum_{i=1}^6 \kappa_{R_i})} \prod_{b=1}^6 \mathcal{W}_{R_{b+1}, R_b} \tag{72}$$

Where

$$l_H = l_1 + l_3 + l_5, \quad l_{E_1} = l_1 + l_3 - l_2, \quad l_{E_2} = l_3 + l_5 - l_4, \quad l_{E_3} = l_1 + l_5 - l_6. \tag{73}$$

E_a : In this case we have to take $l_1 = l_3 = l_5 = 0$ and $l_a = \delta_{a,2} + \delta_{a,4} = \delta_{a,6}$.

$$\begin{aligned}
\mathcal{I}(E_a) &= -e^{-T_{E_a}}, \mathcal{W}_{\square}^2, \\
&= \frac{e^{-T_{E_a}}}{(2\sin(g_s/2))^2}.
\end{aligned} \tag{74}$$

Thus we get as expected $N_{E_a}^g = \delta_{g,0}$.

$H - E_a - E_b, a \neq b$: In this case we have only one term contributing for each curve. For $H - E_1 - E_3$ we have $l_a = (0, 0, 1, 0, 0, 0)$, for $H - E_1 - E_3$ we have $l_a = (0, 1, 0, 0, 0, 0)$ and for $H - E_2 - E_3$ we have $l_a = (1, 0, 0, 0, 0, 0)$. Thus we get

$$\begin{aligned}
\mathcal{I}(H - E_a - E_b) &= -e^{-(T_H - T_{E_a} - T_{E_b})} \mathcal{W}_{\square}^2, \\
&= \frac{e^{-(T_H - T_{E_1} - T_{E_2})}}{(2\sin(g_s/2))^2}.
\end{aligned} \tag{75}$$

Thus again we get the correct result $N_{H-E_a-E_b}^g = \delta_{g,0}$.

5.5 $F_0 = \mathbb{P}^1 \times \mathbb{P}^1$

This case was discussed in detail in [21]. We include this here for completeness. The web diagram is shown in Fig. 14 from which we get the following $SL(2, \mathbf{Z})$ matrices associated with the vertices.

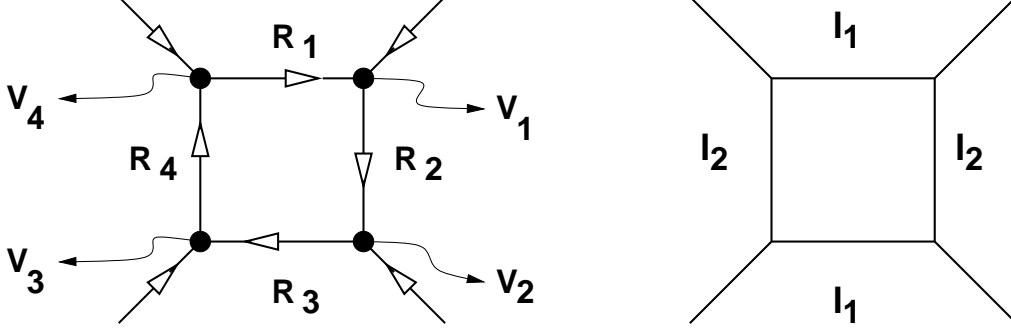


Figure 14: 5-brane web dual to local $\mathbb{P}^1 \times \mathbb{P}^1$.

$$\begin{pmatrix} 1 \\ 0 \end{pmatrix} \xrightarrow{\mathcal{V}_1} \begin{pmatrix} 0 \\ -1 \end{pmatrix} \xrightarrow{\mathcal{V}_2} \begin{pmatrix} -1 \\ 0 \end{pmatrix} \xrightarrow{\mathcal{V}_3} \begin{pmatrix} 0 \\ 1 \end{pmatrix} \xrightarrow{\mathcal{V}_4} \begin{pmatrix} 1 \\ 0 \end{pmatrix}, \quad (76)$$

$$\mathcal{V}_1 = \mathcal{V}_2 = \mathcal{V}_3 = \mathcal{V}_4 = S^{-1}.$$

The amplitude associated with it is then given by

$$e^{F_{inst}^{(c)}} = \sum_{a=1}^4 \sum_{R_a} e^{-\sum_{a=1}^4 l_a r_a} \prod_{b=1}^4 \langle R_{b+1} | \mathcal{V}_{b+1} | R_b \rangle. \quad (77)$$

Where we have $R_5 = R_1$ and $\mathcal{V}_5 = \mathcal{V}_1$. This is exactly the expression obtained in [21] using geometric transition of F_0 blown up at four points. The relation between the renormalized Kähler parameters and $r_{1,2}$ can be obtained from the terms with only one l_a non-vanishing.

$$\underline{l_a = \delta_{ab}}$$

$$\begin{aligned} I_b &= e^{-r_b} W_{\square}^2, \\ &= e^{-r_b} \left(\frac{\lambda^{1/2} - \lambda^{-1/2}}{q^{1/2} - q^{-1/2}} \right)^2. \end{aligned} \quad (78)$$

Thus $\lambda \mapsto \infty$ limit implies that we have to define the renormalized T_{l_1} and T_{l_2} as follows

$$\begin{aligned} r_1 = r_3 &= T_{l_1} + \log(\lambda), \\ r_2 = r_4 &= T_{l_2} + \log(\lambda). \end{aligned} \quad (79)$$

Here $l_{1,2}$ are the two \mathbb{P}^1 such that

$$l_a \cdot l_b = 1 - \delta_{ab}. \quad (80)$$

5.6 F_2

Now consider the case of local CY manifold which has compact divisor F_2 , the second Hirzebruch surface. We consider this cases since it would be difficult to analyze using the geometric transition technique [21, 20]. The toric diagrams are shown in Fig. 8 from which we can obtain the the web diagram as shown in Fig. 15. In this case also to begin with we have to determine which curve classes C_a correspond to the four internal lines of the web diagram.

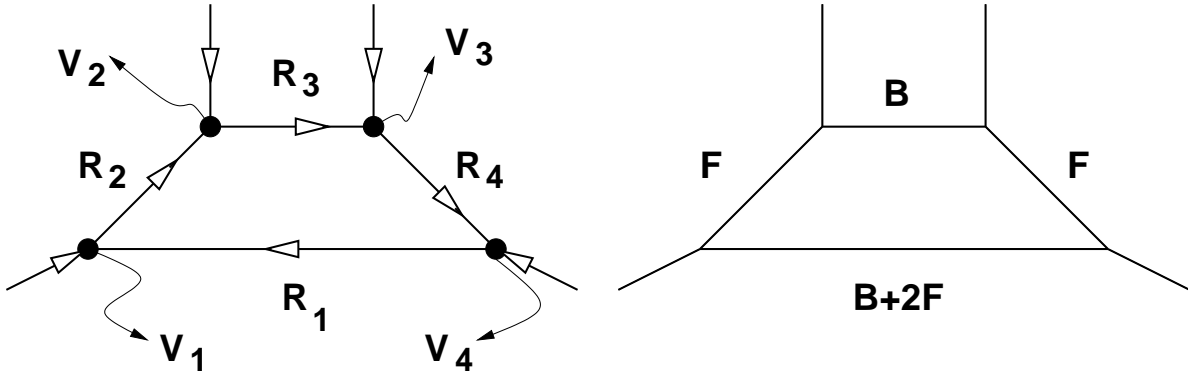


Figure 15: 5-brane web dual to local F_2 .

Homology, Kähler parameters, gluing matrices and the Riemann surface: Second Hirzebruch surface F_2 like F_0 and $B_1 = F_1$ is a \mathbb{P}^1 bundle over \mathbb{P}^1 and has a two dimensional second homology group spanned by the class of the base \mathbb{P}^1 and the class of the fiber \mathbb{P}^1 which we denote with B and F respectively. The class dual to the first Chern class is given by $2B + 4F$ and the intersection numbers are given by

$$B \cdot B = -2, \quad B \cdot F = 1, \quad F \cdot F = 0. \quad (81)$$

From the web diagram it is clear that the curve between the two vertices with parallel external legs is a curve of self-intersection -2 and therefore $C_3 = B$. Also it is clear that $C_2 = C_4 = F$ since F is the only rational curve which intersects B at one point. Since $\sum_{a=1}^4 C_a = 2B + 4F$ (class dual to the first Chern class) thus $C_1 = B + 2F$.

Form Fig. 15 we can easily determine the gluing matrices as the $SL(2, \mathbf{Z})$ matrix associated with a vertex which maps an incoming internal line into the outgoing internal line at that vertex. With the orientation of the lines as shown in Fig. 15 we get

$$\mathcal{V}_1 = TS^{-1}, \quad \mathcal{V}_2 = S^{-1}T^{-1}, \quad \mathcal{V}_3 = T^{-1}S^{-1}, \quad \mathcal{V}_4 = S^{-1}T. \quad (82)$$

The web diagram also completely determines the equation of the Riemann surface obtained by thickening the web. As discussed before the theory on the M5-brane wrapped on this

Riemann surface is dual to the $N = 2$ theory obtained by compactifying Type IIA string theory on the local F_2 . The equation for the Riemann surface for the local F_2 case is given by

$$1 + e^u + e^v + e^{-t_1-u} + e^{-t_2-2u-v} = 0. \quad (83)$$

Where $t_{1,2}$ are Kähler parameters and $u, v \in \mathbb{C}$.

Topological string amplitude and renormalized Kähler parameter: Using the above gluing matrices one can immediately write down the closed string topological amplitude by interpreting the Riemann surface associated with the above web diagram as a Feynman digram with operators \mathcal{V}_a giving the interactions at the vertices.

$$\begin{aligned} e^{F(c)} &= \sum_{R_a} e^{-\sum_{a=1}^4 l_a r_a} \langle R_1 | \mathcal{V}_4 | R_4, 0 \rangle \langle R_4 | \mathcal{V}_3 | R_3, 0 \rangle \langle R_3 | \mathcal{V}_2 | R_2, 0 \rangle \langle R_2 | \mathcal{V}_1 | R_1, 0 \rangle, \\ &= \sum_{R_a} e^{-\sum_{a=1}^4 l_a r_a} \langle R_1 | S^{-1} T | R_4 \rangle \langle R_4 | T^{-1} S^{-1} | R_3 \rangle \langle R_3 | S^{-1} T^{-1} | R_2 \rangle \langle R_2 | T S^{-1} | R_1 \rangle. \end{aligned} \quad (84)$$

To determine the renormalized Kähler parameters T_B, T_F in terms of r_a we determine terms with only one l_a non-vanishing.

$l_a = \delta_{ab}$: we denote this term by \mathcal{I}_b and it is the coefficient of e^{-r_b} in Eq(85),

$$\begin{aligned} \mathcal{I}_b &= e^{-r_b} \langle \square | S^{-1} | 0 \rangle \langle 0 | S^{-1} | \square \rangle, \\ &= -e^{-r_b} \left(\frac{\lambda^{1/2} - \lambda^{-1/2}}{2\sin(g_s/2)} \right)^2, \\ &= \frac{e^{-T_b}}{(2\sin(g_s/2))^2}. \end{aligned} \quad (85)$$

Where in the last line we have taken the limit $\lambda \mapsto \infty$ after defining the renormalized Kähler parameter T_{C_b} associated with the curve C_b such that

$$r_b = T_{C_b} + \log(\lambda). \quad (86)$$

Thus we get the following relations between r_a and T_{C_a} ,

$$\begin{aligned} r_1 &= T_{B+2F} + \log(\lambda) = T_B + 2T_F + \log(\lambda) \\ r_2 &= T_F + \log(\lambda), \\ r_3 &= T_B + \log(\lambda), \\ r_4 &= T_F + \log(\lambda). \end{aligned} \quad (87)$$

5.6.1 Integer invariants for few curves classes

Using the above relations we can write Eq(85) in terms of $T_{B,F}$,

$$e^{F_{inst}^{(c)}} = \sum_{R_a} e^{-(l_1+l_3)T_B-(2l_1+l_2+l_4)T_F} \mathcal{W}_{R_1,R_4} \mathcal{W}_{R_4,R_3} \mathcal{W}_{R_3,R_2} \mathcal{W}_{R_2,R_1}. \quad (88)$$

Where as before $\mathcal{W}_{R_a,R_b}(q)$ is the coefficient of the leading power of λ in $\langle \bar{\square} | S^{-1} | 0 \rangle$.

We calculate the integer invariants associated with B, F and $B + F$. The term contributing to C we denote by $\mathcal{I}(C)$,

$$\begin{aligned} \mathcal{I}(B) &= e^{-T_B} \mathcal{W}_{\square}^2, \\ &= -\frac{e^{-T_B}}{(2\sin(g_s/2))^2}. \end{aligned} \quad (89)$$

This gives $N_B^g = -\delta_{g,0}$. For F we get

$$\begin{aligned} \mathcal{I}(F) &= e^{-T_F} 2\mathcal{W}_{\square}^2, \\ &= -\frac{2e^{-T_F}}{(2\sin(g_s/2))^2}. \end{aligned} \quad (90)$$

Which gives $N_F^g = -2\delta_{g,0}$ as expected since the moduli space of F is just the base curve B which is a \mathbb{P}^1 . Since we want to determine the expansion up to $e^{-T_B-2T_F}$ therefore we need to determine also the term $\mathcal{I}(2F)$,

$$\begin{aligned} \mathcal{I}(2F) &= e^{-2T_F} \{2\mathcal{W}_{\square\square}^2 + 2\mathcal{W}_{\square}^2 + \mathcal{W}_{\square}^4\}, \\ &= e^{-2T_F} \frac{q^{-1} + 2 + q}{(q^{1/2} - q^{-1/2})^4 (q^{1/2} + q^{-1/2})^2}. \end{aligned} \quad (91)$$

Now consider the curve $B + F$.

$$\begin{aligned} \mathcal{I}(B + F) &= e^{-T_B-T_F} 2\mathcal{W}_{\square}^2 \mathcal{W}_{\square,\square}, \\ &= -\frac{2e^{-T_B-T_F}}{(2\sin(g_s/2))^2} + \frac{2e^{-T_B-T_F}}{(2\sin(g_s/2))^4}. \end{aligned} \quad (92)$$

Finally the term associated with $B + 2F$ is

$$\begin{aligned} \mathcal{I}(B + 2F) &= e^{-T_B-2T_F} \{\mathcal{W}_{\square}^2 + 2\mathcal{W}_{\square}(\mathcal{W}_{\square,\square}\mathcal{W}_{\square\square} + \mathcal{W}_{\square,\square}\mathcal{W}_{\square}) + \mathcal{W}_{\square}^2\mathcal{W}_{\square,\square}^2\}, \\ &= e^{-T_B-2T_F} \frac{10 - (q + q^{-1}) - 4(q^2 + q^{-2}) + 4(q^3 + q^{-3})}{(q^{1/2} - q^{-1/2})^6 (q^{1/2} + q^{-1/2})^2} \end{aligned} \quad (93)$$

$$\begin{aligned}
F_{inst}^{(c)} &= \log(1 + \mathcal{I}(B) + \mathcal{I}(F) + \mathcal{I}(2F) + \mathcal{I}(B+F) + \mathcal{I}(B+2F) + \dots), \quad (94) \\
&= \mathcal{I}(B) + \mathcal{I}(F) + \{\mathcal{I}(2F) - \frac{1}{2}\mathcal{I}(F)^2\} + \{\mathcal{I}(B+F) - \mathcal{I}(B)\mathcal{I}(F)\} \\
&\quad + \{\mathcal{I}(B+2F) - \mathcal{I}(B+F)\mathcal{I}(F) + \mathcal{I}(B)\mathcal{I}(F)^2 - \mathcal{I}(B)\mathcal{I}(2F)\} + \dots \\
&= -\frac{e^{-T_B}}{(2\sin(g_s/2))^2} - 2\left(\frac{e^{-T_F}}{(2\sin(g_s/2))^2} + \frac{e^{-2T_F}}{2(2\sin(g_s))^2}\right) - \frac{2e^{-T_B-T_F}}{(2\sin(g_s/2))^2} \\
&\quad - \frac{4e^{-T_B-2T_F}}{(2\sin(g_s/2))^2} + \dots
\end{aligned}$$

Thus we get $N_{B+F}^g = -2\delta_{g,0}$ and $N_{B+2F}^g = -4\delta_{g,0}$ as expected [7].

5.7 F_2 blown-up at one point

The web diagram in this case is given by Fig. 16 from which we can immediately write down the $SL(2, \mathbf{Z})$ matrices associated with the vertices.

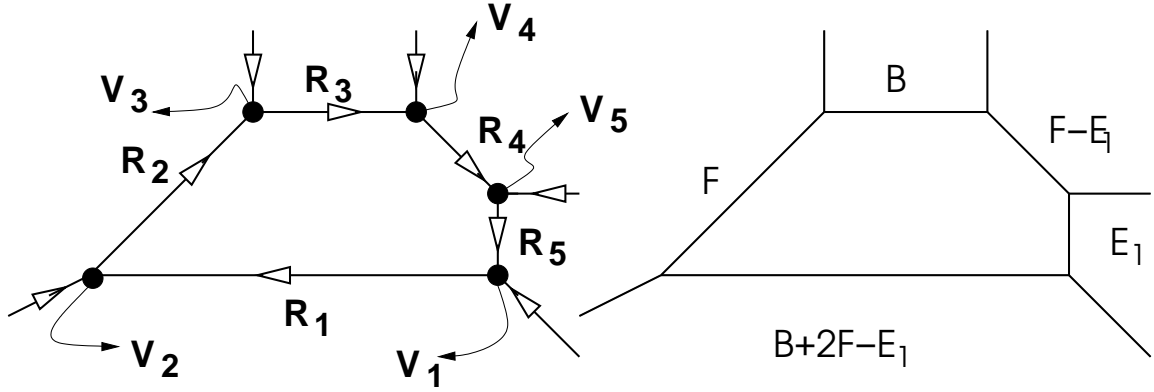


Figure 16: 5-brane web of the local F_2 blown-up at one point.

$$\mathcal{V}_1 = T^{-1}S^{-1}, \quad \mathcal{V}_2 = TS^{-1}, \quad \mathcal{V}_3 = S^{-1}T^{-1}, \quad \mathcal{V}_4 = T^{-1}S^{-1}, \quad \mathcal{V}_5 = TS^{-1}. \quad (95)$$

The amplitude is given by,

$$e^{F_{inst}^{(c)}} = \sum_{a=1}^5 \sum_{R_a} e^{-\sum_{b=1}^5 l_b r_b} \prod_{b=1}^5 \langle R_{b+1} | \mathcal{V}_{b+1} | R_b \rangle. \quad (96)$$

Where $R_6 = R_1$ and $\mathcal{V}_6 = \mathcal{V}_1$. By calculating the terms with $l_a = \delta_{ab}$ we can determine the renormalized; Kähler parameters in terms of r_b ,

$$r_1 = T_B + 2T_F - T_{E_1} + \log(\lambda), \quad (97)$$

$$\begin{aligned}
r_2 &= T_F + \log(\lambda), \\
r_3 &= T_B + \log(\lambda), \\
r_4 &= T_F - T_{E_1} + \log(\lambda), \\
r_5 &= T_{E_1} + \log(\lambda).
\end{aligned}$$

In terms of the renormalized Kähler parameters the amplitude is given by,

$$e^{F_{inst}^{(c)}} = \sum_{a=1}^5 \sum_{R_a} e^{-(l_B T_B - l_F T_F - l_{E_1} T_{E_1})} (-1)^{l_1 + l_4 + l_5} q^{\frac{1}{2}(\kappa_{R_5} - \kappa_{R_4} - \kappa_{R_1})} \prod_{b=1}^5 \mathcal{W}_{R_{b+1}, R_b}. \quad (98)$$

where

$$l_B := l_1 + l_3, \quad l_F := 2l_1 + l_2 + l_4, \quad l_{E_1} = l_1 + l_4 - l_5. \quad (99)$$

We compute the invariants for exceptional curves E_1 and $F - E_1$ to show that the amplitude gives the correct result.

E_1 : Only one term with $(l_1, l_2, l_3, l_4, l_5) = (0, 0, 0, 0, 1)$ contributes,

$$\begin{aligned}
\mathcal{I}(E_1) &= e^{-T_{E_1}} (-1) \mathcal{W}_{\square}^2, \\
&= \frac{e^{-T_{E_1}} (2\sin(g_s/2))^2}{(2\sin(g_s/2))^2} \mapsto N_{E_1}^g = \delta_{g,0}.
\end{aligned} \quad (100)$$

$F - E_1$: In this case also only one term with $l_a = \delta_{a,4}$ contributes,

$$\begin{aligned}
\mathcal{I}(F - E_1) &= e^{-(T_F - T_{E_1})} (-1) \mathcal{W}_{\square}^2, \\
&= \frac{e^{-(T_F - T_{E_1})}}{(2\sin(g_s/2))^2}, \mapsto N_{F-E_1}^g = \delta_{g,0}.
\end{aligned} \quad (101)$$

5.8 F_2 blown-up at two points

The web diagram is shown in Fig. 17 from which we obtain the following $SL(2, \mathbf{Z})$ matrices associated with the vertices

$$\mathcal{V}_1 = T^{-1}S^{-1}, \quad \mathcal{V}_2 = \mathcal{V}_3 = \mathcal{V}_4 = S^{-1}T^{-1}, \quad \mathcal{V}_5 = \mathcal{V}_6 = T^{-1}S^{-1}. \quad (102)$$

The amplitude is then given by,

$$e^{F_{inst}^{(c)}} = \sum_{a=1}^6 \sum_{R_a} e^{-\sum_{b=1}^6 l_b r_b} \prod_{b=1}^6 \langle R_{b+1} | \mathcal{V}_{b+1} | R_b \rangle. \quad (103)$$

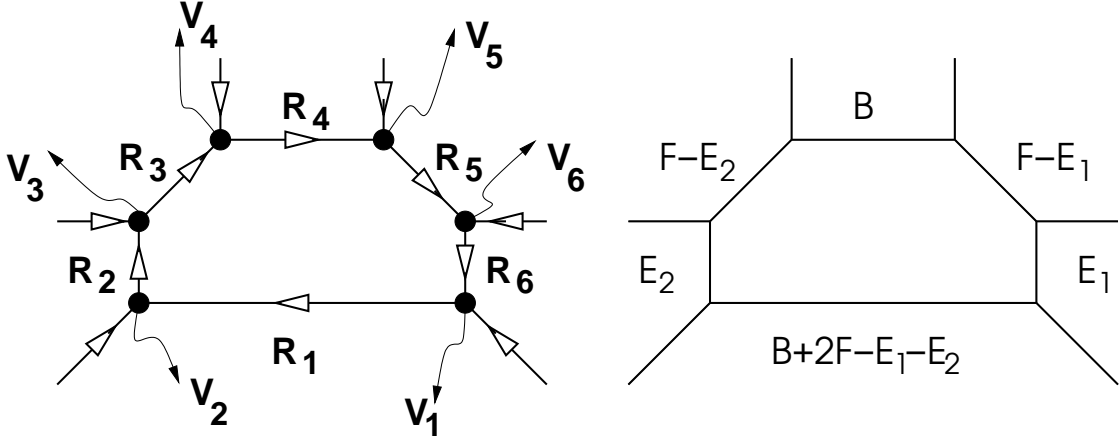


Figure 17: 5-brane web dual to the local F_2 blown-up at two points.

Where $R_7 = R_1$ and $\mathcal{V}_7 = \mathcal{V}_1$. By calculating the terms with $l_a = \delta_{ab}$ we can determine the renormalized Kähler parameters in terms of r_b ,

$$\begin{aligned}
r_1 &= T_B + 2T_F - T_{E_1} - T_{E_2} + \log(\lambda), \\
r_2 &= T_{E_2} + \log(\lambda), \\
r_3 &= T_F - T_{E_2} + \log(\lambda), \\
r_4 &= T_B + \log(\lambda), \\
r_5 &= T_F - T_{E_1} + \log(\lambda), \\
r_6 &= T_{E_1} + \log(\lambda).
\end{aligned} \tag{104}$$

In terms of T_{B,F,E_1,E_2} the amplitude is given by

$$e^{F_{inst}^{(c)}} = \sum_{a=1}^6 \sum_{R_a} e^{-(l_B T_B + l_F T_F - l_{E_1} T_{E_1} - l_{E_2} T_{E_2})} (-1)^{l_2 + l_3 + l_5 + l_6} q^{-\frac{1}{2}(2\kappa_{R_1} + \kappa_{R_2} + \kappa_{R_3} + \kappa_{R_5} + \kappa_{R_6})} \prod_{b=1}^6 \mathcal{W}_{R_{b+1}, R_b}.$$

where

$$l_B := l_1 + l_4, \quad l_F := 2l_1 + l_3 + l_5, \quad l_{E_1} := l_1 + l_5 - l_6, \quad l_{E_2} := l_1 + l_3 - l_2. \tag{105}$$

6 Conclusions

We have seen that topological closed string amplitudes can be written down directly from the web diagram although underlying reason for a such a simple description of these amplitudes is still a mystery. It would be extremely interesting to find this underlying theory giving the

propagator and the three point vertex not only because it would give important insight into closed string amplitudes but it may also provide a simple way of computing all genus open string amplitudes. We believe that open string amplitudes also have a similar description in terms of 5-brane webs with extra ingredient that we insert an operator in the calculation of amplitude corresponding to the 3-cycle on which the holomorphic curves can have boundaries as discussed in [37, 38].

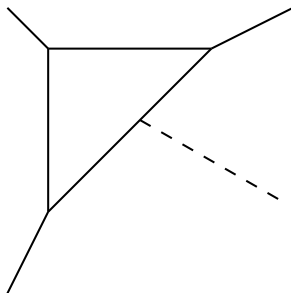


Figure 18: Dashed line represents the non-compact 3-cycles on which D6-brane is wrapped.

Acknowledgments

I would like to thank Jacques Distler, Vadim Kaplunovsky and Cumrun Vafa for valuable discussions. This research was supported by NSF grant PHY-0071512.

References

- [1] M. Bershadsky, S. Cecotti, H. Ooguri, C. Vafa, “Kodaira-Spencer Theory of Gravity and Exact Results for Quantum String Amplitudes,” *Commun. Math. Phys.* **165** (1994) 311-428.
- [2] M. Gromov, “ Pseudo-holomorphic Curves on Almost Complex Manifolds,” *Invent. Math.* **82** (1985) 307-347.
- [3] E. Witten, “Topological Sigma Models,” *Commun. Math. Phys.* **118** (1988) 411-449.
- [4] P. S. Aspinwall, D. Morrison, “Topological Field Theory and Rational Curves,” *Commun. Math. Phys.* **151** (1993) 245-262, [hep-th/9110048](#).
- [5] E. Witten, “Mirror Manifolds and Topological Field Theory,” [hep-th/9112056](#).

- [6] T. -M. Chiang, A. Klemm, S. -T. Yau, E. Zaslow, “Local Mirror Symmetry: Calculation and Interpretations,” *Adv. Theor. Math. Phys.* **3** (1999) 495-565, [hep-th/9903053](#).
- [7] A. Klemm, E. Zaslow, “Local Mirror Symmetry at Higher Genus,” [hep-th/9906046](#).
- [8] D. Ghoshal, C.Vafa, “c=1 String as the Topological Theory of the Conifold,” *Nucl. Phys.* **B453** 121-128, [hep-th/9506122](#).
- [9] S. Katz, A. Klemm, C. Vafa, “M-Theory, Topological Strings and Spinning Black Holes,” *Adv. Theor. Math. Phys.* **3** (1999) 1445-1537, [hep-th/9910181](#).
- [10] R. Gopakumar, C. Vafa, “M-Theory and topological strings-II,” [hep-th/9812127](#).
- [11] H. Ooguri, C. Vafa, “Knot invariants and topological strings,” *Nucl. Phys.* **B 577** (2000) 419, [hep-th/9912123](#).
- [12] R. Gopakumar, C. Vafa, “On the gauge theory/geometry correspondence,” *Adv. Theor. Math. Phys.* **3** (1999) 1415, [hep-th/9811131](#).
- [13] H. Ooguri, C. Vafa, “Worldsheet Derivation of a Large N Duality,” [hep-th/0205297](#).
- [14] J. M. F. Labastida, M. Mariño, “Polynomial invariants for torus knots and topological strings,” *Commun. Math. Phys.* **217** (2001) 423-449, [hep-th/0004196](#).
- [15] P. Ramadevi, T. Sarkar, “On Link Invariants and Topological String Amplitudes,” *Nucl. Phys.* **B600** (2001) 487-511, [hep-th/0009188](#).
- [16] J. M. F. Labastida, M. Mariño, C. Vafa, “Knots, links and branes at large N ,” *JHEP* **0011** (2000) 007, [hep-th/0010102](#).
- [17] S. Sinha, C. Vafa, “SO and Sp Chern-Simons at large N ,” [hep-th/0012136](#).
- [18] A. Iqbal, A. -K. Kashani-Poor, in progress.
- [19] M. Mariño, C. Vafa, “Framed knots at large N ,” [hep-th/0108064](#).
- [20] D. -E. Diaconescu, B. Florea, A. Grassi, “Geometric Transitions and Open String Instantons,” [hep-th/0205234](#);
D. -E. Diaconescu, B. Florea, A. Grassi, “Geometric transitions, del Pezzo surfaces and open string instantons,” [hep-th/0206163](#).
- [21] M. Aganagic, M. Mariño, C. Vafa, ”All Loop Topological String Amplitudes From Chern-Simons Theory”, [hep-th/0206164](#).
- [22] E. Witten, “Chern-Simons gauge theory as a string theory,” in *The Floer memorial volume*, Birkhäuser 1995, p.637, [hep-th/9207094](#).

- [23] N. C. Leung, C. Vafa, “Branes and Toric Geometry,” *Adv. Theor. Math. Phys.* **2** (1998) 91-118, [hep-th/9711013](#).
- [24] O. DeWolfe, A. Hanany, A. Iqbal, E. Katz, “Five-branes, Seven-branes and Five-dimensional E_n field theories,” *JHEP* **9903** (1999) 006, [hep-th/9902179](#).
- [25] O. Aharony, A. Hanany, B. Kol, “Webs of (p,q) 5-branes, Five Dimensional Field Theories and Grid Diagrams,” *JHEP* **9801** (1998) 002, [hep-th/9710116](#).
- [26] B. Kol, J. Rahmfeld, “BPS Spectrum of 5 Dimensional Field Theories, (p,q) Webs and Curve Counting,” *JHEP* **9808** (1998) 006, [hep-th/9801067](#).
- [27] G. Bonelli, “The M5-brane on K3 and del Pezzo’s and multi-loop string amplitudes,” *JHEP* **0112** (2001) 022, [hep-th/0111126](#).
- [28] R. Dijkgraaf, E. Verlinde, M. Vonk, “On the partition sum of the NS five-brane,” [hep-th/0205281](#).
- [29] K. Hori, C. Vafa, “Mirror Symmetry,” [hep-th/0002222](#),
- [30] K. Hori, A. Iqbal, C. Vafa, “D-branes and Mirror Symmetry,” [hep-th/0005247](#).
- [31] E. Witten, “Phases of $N = 2$ Theories In Two Dimensions,” *Nucl. Phys.* **B403** (1993) 159-222, [hep-th/9301042](#).
- [32] E. Verlinde, “Fusion rules and modular transformations in 2-D conformal field theory,” *Nucl. Phys.* **B 300** (1988) 360.
- [33] M. Aganagic, D. -E. Diaconescu, A. Grassi, M. Mariño, C. Vafa, To appear.
- [34] E. Witten, “Quantum field theory and the Jones polynomial,” *Commun. Math. Phys.* **121** (1989) 351.
- [35] H. R. Morton, S. G. Lukac, “The HOMFLY polynomial of the decorated Hopf link,” [math.GT/0108011](#).
- [36] S. G. Lukac, “HOMFLY skeins and the Hopf link,” Ph.D Thesis, June 2001, in <http://www.liv.ac.uk/~su14/knotgroup.html>
- [37] M. Aganagic, C. Vafa, “Mirror Symmetry, D-Branes and Counting Holomorphic Discs,” [hep-th/0012941](#).
- [38] M. Aganagic, A. Klemm, C. Vafa, “Disk instantons, mirror symmetry and the duality web,” *Z. Naturforsch.* **A 57** (2002) 1, [hep-th/0105045](#).